DENTAL IMPLANT STABILITY ANALYSIS BY USING RESONANCE FREQUENCY METHOD

By

Reza Harirforoush
M. Sc., Islamic Azad University, Tehran South Branch 2003
B. Sc., Islamic Azad University, Tehran Central Branch 2001

THESIS SUBMITTED IN PARTIAL FULFILLMENT OF
THE REQUIREMENTS FOR THE DEGREE OF

MASTER OF APPLIED SCIENCE

In the
School of Engineering Science
Faculty of Applied Sciences

SIMON FRASER UNIVERSITY

Summer 2012

APPROVAL

Name: **Reza Harirforoush**

Degree: **Master of Applied Science**

Title of Thesis: **Dental Implant Stability Analysis by using Resonance Frequency Method**

Examining Committee:

Chair: **Dr. M. Moallem**

Associate Professor of Engineering Science

_____

Dr. Siamak Arzanpour
Senior Supervisor
Assistant Professor of Engineering Science

_____

Dr. G.Wang
Supervisor
Professor of Engineering Science

_____

Dr. Woo Soo Kim
Internal Examiner
Assistant Professor of Engineering Science

Date Defended/Approved: July 26, 2012

Partial Copyright Licence

ABSTRACT

The use of dental implants in the rehabilitation of partially and completely edentulous patients has been significantly increased in recent years. Although high survival rates of implants supporting prosthesis have been reported, failure still happens due to bone loss as results of primary and secondary implant stability. Primary stability of an implant mostly comes from mechanical interaction with cortical bone while secondary stability happens through bone regeneration and remodelling at the implant/bone interface. Defining the implant stability remains a challenge in dentistry and several researches have been made in this field. To detect implant stability, various diagnosis analyses have been employed. Among them, resonance frequency analysis (RFA) is an objective method of monitoring implant/tissue integration.

In this thesis, experimental and numerical studies are carried out to find the effect of some parameters affecting the stability of dental implant by using RFA. Modal analysis technique is employed to investigate the effect of coupled mode shapes in dental implant. Moreover, the primary stability of dental implant that indicates the process of bone-implant integration is investigated. Resonance frequency of jaw-implant structure is carried out using finite element modelling. Different implant-bone interface conditions are studied for this investigation. The effects of endosseous implant angulation on the resonance frequency of implant are studied. MIMICS, a three dimensional (3D) modelling software was used to construct a 3D model of a pig mandible from computed tomography (CT) images. The resonance frequency of the implant was analyzed using finite element (FE) modal analysis in a simulated environment. The MIMICS is also used to investigate effect of soft tissue surrounding the implant on the RF of implant. In addition, three different pig mandibles were employed to assess the effect of some parameters affecting resonance frequency of implant. Finally, experimental studies are carried out to investigate the effect of soft tissue on RF of implant. A novel device is also designed for stability analysis of dental implants.

Keywords: Implant stability, resonance frequency, modal analysis, finite element method, MIMICS

ACKNOWLEDGEMENTS

In the name of Allah, the Most Gracious and the Most Merciful

It would not have been possible to write this M.Sc. thesis without the help and support of the kind people around me, to only some of whom it is possible to give particular mention here. This thesis would not have been possible without the help, support and advice of my supervisor, Prof. S. Arzanpour. I have been extremely lucky to have a supervisor who cared so much about my work, and who responded to my questions and queries so promptly. His positive and friendship personality has continually inspired me. The good advice and support of my UBC supervisor, Dr. B. Chehroudi, has been invaluable on both an academic and a personal level, for which I am extremely grateful. I also thank the Department of MSE for their support and assistance especially the head of department, Prof. F. Golnaraghi. The library facilities and computer facilities of the SFU have been indispensable. I would like to thank Prof. Carolyn Sparrey for her kindness; friendship and support to allow me using MIMICS software. I would also like to thank my colleagues and friends in the Dental Engineering Lab, E. Asadi, Ciara and V. Zakeri, H. Dehghani.

Above all, I deeply would like to thank my lovely wife, Mahsa, for her personal support and great patience at all times. My parents, brother, brothers in law, sister and sisters in law have given me their unequivocal support throughout, as always, for which my mere expression of thanks likewise does not suffice.

TABLE OF CONTENTS

LIST OF FIGURES

LIST OF TABLES

NOMENCLATURE

m	Mass
c	Damper
k	Stiffness
$H(\omega)$	Frequency response function
[M]	Mass matrix
[C]	Damping matrix
[K]	Stiffness matrix
P	Normalized eigenvectors
l	Length
I	moment of inertia
E	Modulus f elasticity
ρ	density
d_j^i	Absolute difference

Greek symbols

ω	Natural frequency
ω_0	Undamped natural frequency
ξ	critical damping ratio
$\alpha(\omega)$	receptance matrix
f	Resonance frequency
β	Constant
ϑ	Poisson`s ratio
ω_d	Damped natural frequency

Subscript

CRA	Cutting Torque resistant Analysis
RTT	Reverse Torque Test
RTV	Reverse Torque Value
POWF	Pulse Oscillation Wave Form
FFT	Fast Fourier Transform
DMC	Dental Mobility Checker
CT	Contact Time / Computed Tomography
RFA	Resonance Frequency Analysis
DOF	Degree of Freedom
RF	Resonance Frequency
ISQ	Implant Stability Quotient
FEA	Finite Element Analysis
FE	Finite Element

FEM	Finite Element Method
QUS	Quantitative Ultrasound
CCBR	Cortical to Cancellous Bone Ratio
SDOF	Single Degree of Freedom
MDOF	Multi Degree of Freedom
FRF	Frequency Response Function
CBCT	Cone Beam Computed Tomography
RP	Reference Point
RCS	Reference Coordinate System

1: INTRODUCTION

The use of dental implants in the rehabilitation of partially and completely edentulous patients has been significantly increased in dentistry since 1980 [1]. Although high survival rates of implants supporting prosthesis have been reported [2,3,4], failure still happens due to bone loss as a results of primary and secondary implant stability. Primary stability of an implant is the absence of mobility in the bone bed upon insertion of the implant and mostly comes from mechanical interaction with cortical bone. It is also named as "Mechanical Stability" which is the result of compressed bone holding the implant tightly in the bone. Secondary stability, named as "Biological Stability", happens through bone regeneration and remodelling at the implant/bone interface [5,6]. It is the result of new bone cells forming at the site of the implant and osseointegration. The primary stability is the requirement for successful secondary stability [6]. Secondary stability orders the time of functional loading [7]. Following the placement of an endosseous implant, primary mechanical stability gradually decreases and secondary stability (biologic) gradually increases.

Bone quantity and quality, surgical techniques including the skill of the surgeon, implant (geometry, length, diameter, and surface characteristics) are major factors affecting primary stability [8]. Primary stability, bone modelling and remodelling, and implant surface conditions are the main parameters influencing secondary stability [8].

Osseointegration is an important factor in specifying a series of criteria that identifies success or failure of an implant. Osseointegration is, however, a patient-dependent wound healing process that happens at two different stages: primary stability and secondary stability.

Dental implant stability measurement, an indirect indication of osseointegration, is a measurement of implant's resistance to movement [9]. Objective measurement of implant stability is a valuable tool for achieving consistently good results first and foremost because implant stability plays such an important role in achieving a

successful outcome. The advantages of measuring implant stability are to make more accurate decisions about the time of crown loading or unloading, select the protocol of choice for implant loading, and increase trust between patient and practitioner. It is, therefore important to be able to quantify implant stability at various times and have in place a long-term prognosis based on implant stability measurement tool. Although various diagnosis analyses have been employed and several research and development projects have been already made in this field, measuring implant stability remains a challenge in dentistry.

1.1 Available methods currently used to assess implant stability

In this section, the currently available methods to evaluate implant stability are discussed. The methods for studying stability can be categorized as invasive, which interfere with the osseointegration process of the implant, and non-invasive, which do not. Some of the most famous methods in analyzing dental implant stability are histologic analysis, percussion test, radiographs, reverse torque, cutting resistance, and resonance frequency analysis (RFA). Since histologic analysis is not feasible for daily practice it is not discussed in this chapter.

1.1.1 Radiographic analysis

Radiographic analysis was one of the first methods applied to evaluate the condition of implants after they had been placed. Radiographic evaluation is a non-invasive method that can be performed at any stage of healing process. Bitewing radiographs are used to measure crestal bone level, defined as the distance from the top of the implant to the position of the bone on the implant surface, because it has been suggested as an indicator for implant success [10]. However, other studies recommended that the resolution of bitewing radiographs cannot be used as the only tool to evaluate either primary or secondary stability [8]. Moreover, crestal bone changes can be only reliably measured if there is no distortion in the radiographic pictures. In those pictures, the distortion happens when the central x-ray tube is not positioned parallel to the implant. Furthermore, panoramic view (a dental X-ray scanning of the upper and lower

jaw that shows a two-dimensional view of a half circle from ear to ear) does not provide information on a facial bone level, and bone loss. Finally, regular radiographs cannot be used to quantify neither bone quality nor density. They can be used to assess changes in bone mineral only when there are decreases that exceed 40% of the initial mineralization [11]. Moreover, because of X-radiation hazards other methods with fewer side effects are preferred.

1.1.2 Cutting Torque Resistance Analysis (CRA)

This method was originally developed in 1994 by Johansson and Strid [12] and later improved *in vitro* and *in vivo* human models. In this method the energy ($\frac{J}{mm^3}$) required in cutting off a unit volume of bone during implant surgery is measured. This energy has been shown to be significantly correlated with bone density, which has been suggested as one factor that significantly influences implant stability [13]. The advantages of this method are detecting bone density and its quality during surgery. The major limitation of CRA is that it does not give any information on bone quality until the osteotomy site (a surgical operation for bone shortening or realignment) is prepared. In addition, this information cannot be used to assess bone quality changes after implant insertion.

1.1.3 Reverse Torque Test (RTT)

The Reverse Torque Test (RTT), which is proposed in 1984 by Roberts *et al*. [14], measures the critical torque threshold when bone-implant contact is broken. This indirectly provides information on the degree of bone-implant contact in a given implant. Removal Torque Value (RTV) as an indirect measurement of bone-implant contact was reported to range from 45 to 48 N.cm [15]. The disadvantage of this method is the risk of irreparable plastic deformation within implant bone integration and the implant failure when unnecessary load is applied to an implant that is still undergoing osseointegration. In addition, applying torque on implants placed in bone of low quality may result in a shearing of bone-to-implant contact and cause implants to irretrievably fail.

1.1.4 Insertion torque analysis

Insertion torque analysis, as an invasive method, expresses the amount of force that is applied to the implant as it is inserted. Implant placement insertion torque is initially minimal, and increases quickly until the cortical layer (see Figure 1-1) in a jawbone is fully engaged. As the implant is driven into the bone, repeated measurements are taken and a graph is often produced. The maximum value is obtained when the head of the screw makes contact with the cortical plate (the hard, outer shell of alveolar). Insertion torque measurement includes finding the maximum insertion torque value when the screw head contacts the cortical plate. This test has been generally well accepted and has been used for evaluating various implant designs [16]. Insertion torque has been found to correlate with bone density and consequently implant stability [17]. The application of insertion torque has been shown to be limited since estimating the quality of the bone is impossible until the implant insertion is actually started. So, insertion torque measurements cannot be used for the selection of implant sites. This method also cannot be used to follow implant healing and osseointegration procedures.

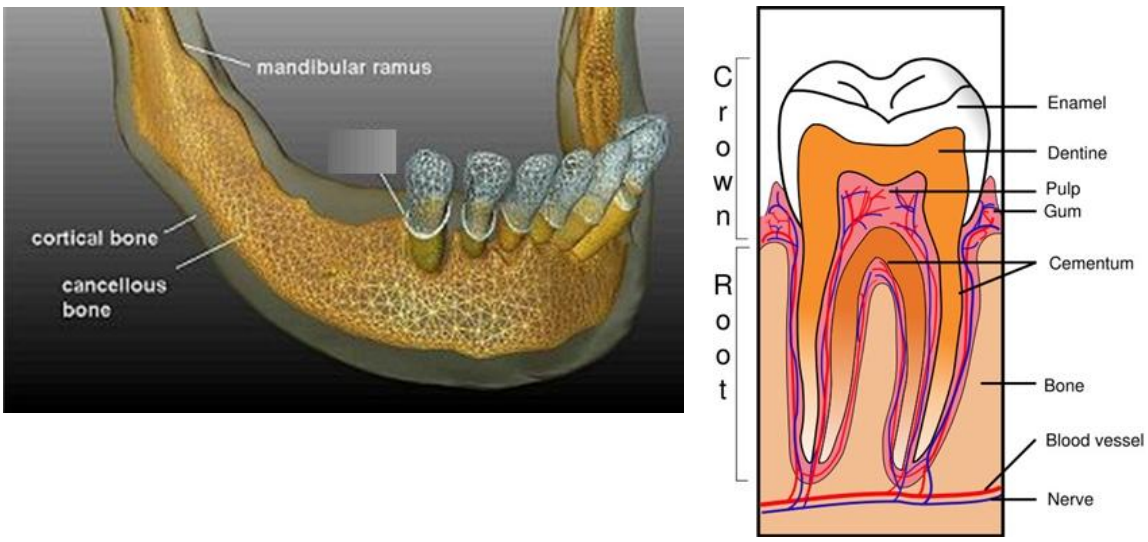

Figure 1-1 : The picture of lower jaw and teeth

1.1.5 Percussion test

Percussion test is the simplest method for testing implant stability. This test is based upon vibrational acoustic science and impact-response theory. In this method,

clinical judgment about osseointegration is made based on the sound heard from the percussion of the implant with a metallic instrument. A “crystal” sound indicates successful osseointegration, while a “dull” sound means weak or failing osseointegration. This method heavily relies on the clinician’s experience level and subjective belief. Therefore, it cannot be used experimentally as a standard testing method.

1.1.6 Pulsed oscillation waveform

Kaneko *et al*. [18,19] used a Pulsed Oscillation Wave Form (POWF) to analyze the mechanical vibrational characteristics of the implant-bone interface using forced excitation of a steady-state wave.

Pulsed oscillation waveform works based on the frequency and amplitude of the implant vibration induced by a small-pulsed force. This system consists of an acoustoelectric driver, an acoustoelectric receiver, a pulse generator and an oscilloscope. Both the acoustoelectric driver and the acoustoelectric receiver consist of a piezoelectric element and a puncture needle. A multifrequency pulsed force of about 1 KHz is applied to the implant by lightly touching it with two fine needles connected to piezoelectric elements. Resonance and vibration generated from the bone-implant interface of an excited implant are picked up and displayed on an oscilloscope. The sensitivity of this method depended on load directions and positions. The sensitivity of this method is low for the assessment of implant rigidity [18].

1.1.7 Impact hammer method

Impact hammer is an example of transient force as a source of excitement. This method is an improved version of the percussion test except that sound generated from contact between hammer and object is processed through fast Fourier transform (FFT). Dental Mobility Checker (DMC; J.Morita, Suita, Japan) and Periotest (Siemens, Bensheim, Germany) are currently available devices working based on impact hammer method.

The DMC was originally developed by Aoki and Hirakawa [20,21]. It detected the level of tooth mobility by converting the integration of teeth and alveolar bone into

acoustic signals. Contac time between the tapping impact hammer and the object is measured. In this theory, the width of the first peak on the time axis of the spectrum generated by transient impulse is inversely proportional to the time axis of the impulse [22]. The lower rigidity of implant-bone integration results in a longer time response. In this device, a microphone is used as a receiver. The response signal of the microphone is processed in the time domain. Some problems were addressed to this method such as difficulties of double tapping and difficulty in obtaining constant excitation.

Unlike the DMC, which applies impact force with a hammer, Periotest uses an electromagnetically driven and electrically controlled metallic tapping rod in a headpiece (see Figure 1-2). Response to striking is then measured by a small accelerometer incorporated into the head of the device. Similar to DMC, the contact time (CT) between the test object and tapping rod is measured in time domain and then converted to a value called PTV, which is related to the damping characteristics of tissue surrounding teeth or implant. For PTV units in the range of -8 to +13, a linear formula is used:

$$\boldsymbol{PTV = \frac{CT}{0.02\ ms} - 21.3} \qquad \textbf{(1)}$$

For PTV values ranging from +13 to +50, a quadratic formula is used:

$$\boldsymbol{PTV = \sqrt{\left(\frac{CT}{0.06\ ms} - 8.493\right)} - 4.17} \qquad \textbf{(2)}$$

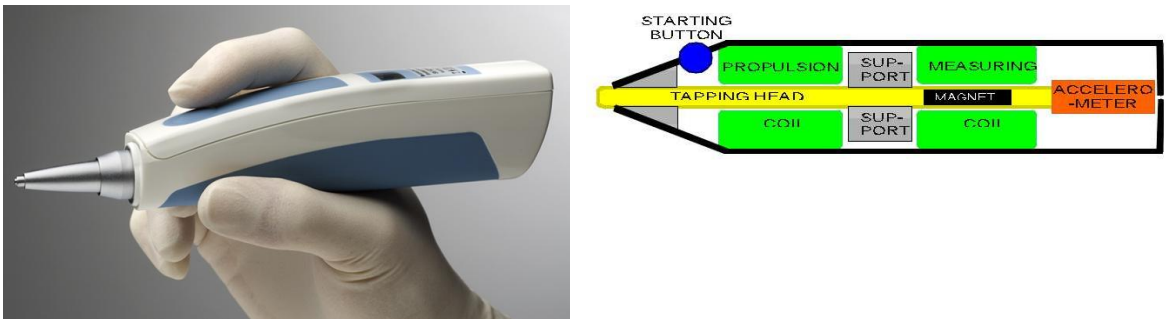

Figure 1-2: Periotest device

The lack of sensitivity is reported as one of the shortcomings of this device [23]. This is because PTV has a very wide dynamic range (PTV is -8 to +50) of possible responses, and the PTV of an osseointegration implant falls only in a relatively narrow zone (-5 to +5) inside the range. Moreover, values measured from Periotest can be

affected by excitation conditions such as position and direction. PTV also cannot be used to identify a "borderline implant" which may or may not be considered as a successful osseointegration. Finally, Periotest measurements are limited because they are strongly dependent to the orientation of the excitation source and the striking point. As a result, despite some positive claims for the Periotest, the prognostic accuracy of the Periotest for implant stability has been criticized for a lack of resolution, poor sensitivity and susceptibility to operator variables [24].

1.1.8 Resonance Frequency Analysis (RFA)

In resonance frequency analysis, implants are forced to oscillate and the frequency at which they oscillate at maximum amplitude is registered as their resonance frequency. Similar to all distributed system, an implant can have many resonance frequencies, each called a harmonic. The resonance frequencies are dependent on the material, length and the quality of the supporting mechanism. Since the material and length of the implant are constants, variations of the resonance frequency highly correlate to the quality of the support (osseointegration).

RFA, as a method of monitoring implant/tissue integration, was first introduced for dental applications in 1996 [25]. It is a non-invasive and objective method for short and long-term monitoring of changes in implant stability [1,26,27]. RFA has been applied for implant stability measurement in both humans [28-30] and animals [31-33] (*in vivo*) and *in vitro* [25,34,32]. RFA, as a technique for measuring dental implant stability, has attracted considerable scientific interest in recent years and an increasing number of prominent journal papers are published about it since its first introduction.

The RFA of an implant, as it was briefly mentioned in this section, can be influenced by some factors including implant length, implant diameter, implant geometry, implant surface characteristic and placement position, as well as bone quality, bone quantity, damping effect of marginal mucosa, bone implant contact, effective implant length and connection to transducer.

Currently, there are two commercially available devices used to evaluate the resonance frequency of implants placed into the bone, Implomates (Bio Tech One) and

Osstell (Integration Diagnostics). Their main difference is in the way they excite implants.

The Implomates device (Taipei, Taiwan) has been studied extensively by Huang *et al*. [32,34-37]. This device utilizes an impact force to excite an implant. There is a small electrically driven rod inside the device that produces impact force. The received time response signal is then transferred in frequency spectrum for analysis (range 2 to 20 KHz). The first peak in the frequency spectrum (distinguishable from the noise) indicates the primary resonance frequency of implant. Higher frequency for the primary resonance and the sharpness of that peak indicates a more stable implant.

Osstell measures RF by attaching a metal rod to an implant with screw connection and exciting the rod doing a frequency sweep. The rod is excited by a small magnet that is attached to its top that can be stimulated by magnetic pulses from a handled electronic device (see Figure 1-3). The rod can vibrate in two directions (perpendicular to each other) and thus it has two fundamental resonance frequencies. Implant Stability Quotient (ISQ) is a scale developed by Osstell for implant stability. It converts the resonance frequency values ranging from 3,500 to 8,500 Hz into an ISQ of 0 to 100. A high value indicates greater stability, while a low value indicates instability. Values greater than 65 are recommended as successful implant stability. Even though Osstell is clinically used but there are not much convincing data on the relation between bone-implant interface and ISQ values [8].

Figure 1-3: Osstell Device

Although for clinical applications, Osstell has a better performance than the Periotest [38], both RFA devices still have some uncertainties. Further research is needed to establish higher reliability of these diagnostic devices.

1.1.9 Finite Element Analysis (FEA)

Finite Element Method (FEM) is a numerical technique, which facilitates the RF analysis by providing an interface where a 3D model of an object and its support can be developed and studied. FEM approximates the real structure with a finite number of elements and assigns mechanical properties of objects such as Young's Modulus, the Poisson ratio and density. This method can simulate complex geometric shapes, material properties, and generate various boundary conditions of the real situation, which are difficult to produce in the laboratory. FEM simulation method has the advantage of allowing independent control of each parameter in the Finite Element (FE) models.

The first person who used modal analysis, the study of the dynamic properties of structures (will be explained in more details in chapter 2) together with Finite Element Method in analysis of implant stability was Williams & Williams [39]. Since then, FEM has gradually become an important tool in biomedical research. Wang *et al.* [40] used FEM for calculating RFA to determine the identifiable stiffness range of interfacial tissue (a thin layer surrounding the implant) of dental implants. They found that when the Young's modulus of the interfacial tissue is less than 15 MPa, the resonance frequencies are significantly affected by the interfacial tissue and the influence of other parameters

such as geometry, boundary constraint, and material property of the bone are negligible. One limitation of finite element modelling is that it is a numerical approach based on many assumptions, which might not necessarily realistic to simulate real cases.

1.1.10 Ultrasonic wave propagation

An alternative method to assess implant stability is quantitative ultrasound (QUS), as suggested initially by de Almeida *et al.* [41]. They used the implant as a waveguide and showed a significant correlation between the experimental 1 MHz ultrasonic responses of an aluminum threaded piece and the screwing depth in an aluminum block. They concluded that Ultrasonic waves are sensitive to bone-implant interface properties. In the same study, finite difference numerical simulations depicted an agreement between the 1 MHz ultrasonic response of titanium wave guides and the elastic properties of tissues surrounding the guides. Furthermore, in a recent experimental study by Mathieu *et al.* [42], a 10 MHz ultrasonic device was validated with implants placed in rabbit bone. The amount of bone surrounding prototype cylindrical titanium implants was shown to be significantly correlated with a quantitative indicator deduced from the ultrasonic response to a 10 MHz excitation.

1.2 Contribution

One of the objectives of this research is to investigate the effect of coupled mode shapes in dental implant. The results of this investigation are given in chapter 2. The effect of bone-implant osseointegration is simulated by securing the implant inside a chuck. Modal analysis technique is used to measure the resonance frequencies of implant-chuck coupled structure. The resonance frequencies of a dental implant fixed by a metal chuck and excited by an impulse hammer under various fixing levels are analyzed. Moreover, the resonance frequency of implant, as one of the components of the implant-chuck coupled structure, is also investigated. A noncontact piezoelectric microphone is used to acquire the vibration response of the implant. The coupled structure was also simulated using finite element modelling in ANSYS modal analysis simulation environment.

Both experimental and numerical results show that the resonance frequency of a coupled implant/chuck is influenced by the material property of each individual units as well as the quality of their integration. Based on the results, it is concluded that the resonance frequencies of implant is still present but the values are changed in the coupled structure (placed inside the chuck).

The analysis of primary stability of dental implant that indicates the process of bone-implant integration is another objective of this research which is investigated in chapter 3. This integration is known to happen at the boundary of the bone and dental implant contact surface. The resonance frequency of dental implant is used as the parameter for this investigation due to its high sensitivity to boundary condition variations. In this chapter, RFA of the jaw-implant structure is carried out using finite element modeling. The FEM analyses are conducted in ANSYS modal analysis simulation environment. The FEM model of the structure includes titanium implant, cancellous and cortical bone (cancellous (spongy) and cortical (compact) bone are two types of tissue that form bones). Different implant-bone interface conditions are studied for this investigation. Various boundary conditions were studied to identify natural frequencies of jaw-implant structure. Our analysis shows that the resonance frequency of the implant increases during the healing period and reaches a plateau when the implant-bone interface was fully integrated. The results show that RFA can be suggested as a non-invasive, reliable and accurate diagnostic method for assessment the healing process of dental implants.

The other subject of interest is dental implant angulation. Dental implants are ideally placed in bone in an orientation that allows vertical transfer of occlusal forces (the force exerted on opposing teeth when the jaws are brought into) along their long axis. Nevertheless, optimal situations for implant placement are seldom encountered resulting in implants placement in angulated positions, which may affect their long-term success. The implant angulation is also influenced by several factors including surrounding anatomical structures, occlusion, vector of occlusal forces, aesthetics, prosthetic components, and availability of healthy hard or soft tissues. RF is one objective tool used to monitor stability of the implant tissue integration; however, it is expected that RF changes with alteration in implant orientation in bone and little is known about this effect. The objective followed in chapter 4 is identifying the effects of implant angulation

on the resonance frequency of implant. The purpose of this study is to determine the relation between the dental implant orientation in the bone and the RF of implant. MIMICS, a three dimensional (3D) modelling software is used to construct a 3D model of a pig mandible from computed tomography (CT) images. The RF of the implant is analyzed using finite element (FE) modal analysis in a simulated environment. In addition, a cubical model is also developed in MIMICS to investigate the parameters concerning the relationship between RF changes and implant orientation in a simplified environment. Implant orientation angle altered by increment of one degree until maximum of ten degrees inclination and RF is analysed. Our analysis shows that the RF fluctuation following altering implant orientation is strongly influenced by the contacting cortical to cancellous bone ratio (CCBR) at the implant interface.

The effect of soft tissue surrounding the implant on the RF of implant is another objective of this study. This has been investigated in chapter 5. The aim of this study is to find the effect of soft tissue surrounding the implant on RF. In this study, MIMICS is used to construct a 3D model of a pig mandible (lower jaw) from computed tomography (CT) images. The 3D model of soft tissue is also built in interfacing areas of implant and bone. The RF of the implant is analyzed using finite element modal analysis in a simulated environment. A vigorous parametric study is conducted to disclose the relation between the soft tissue surrounding the implant and the RF of implant. Our analysis reveals that the RF of implant is mainly affected by surrounding soft tissue when the soft tissue is formed in cortical bone. The volume of soft tissue is also a significant factor in changing the RF of implant. This finding implies that the location and the volume of soft tissue in interfacing areas of implant and bone are dominant parameters in changing the RF of dental implant.

In chapter 6, three different pig mandibles are employed to assess the effect of some parameters such as the effect of free length, and the effect of implant size on RF of implant. In this analysis, the implants are buried in the bone and an impulse hammer excites the implant. The vibrating signals are recorded by both an accelerometer attached to the abutment and a microphone. Both impulse force and the vibrating signal response are analysed to obtain the resonance frequency of implant. The results showed that the RF of implant decreases with increasing the length of implant left out of the bone. It is

also showed that the size of implant inserted in jaw strongly influences the RF of implant. The longer implant showed higher RF. No difference in RF of implant is shown when the whole and partial pig mandible are analyzed separately.

Chapter 7 includes the experimental studies of the effect of soft tissue on RF of implant. The implant is fixed by a rotating metal chuck stand. The effect of soft tissue is simulated by rubber. The implant is partially covered by rubber and then placed inside the chuck to represent the local formation of soft tissue at the implant-bone interface. The chuck is rotated from 0^0 to 360^0 in 10^0 increments.

The result showed decrease of the RF of implant when the implant is surrounded by soft tissue. The results also demonstrate that the RF is mainly affected by the angle between the direction of the transient force and the location of the soft tissue.

In summary, the effect of coupled implant/chuck structure on RF of implant is studied. The numerical approach is carried out to investigate the effect of soft tissue and implant angulation on RF of implant. The effect of soft tissue is also analyzed experimentally.

2: THE EFFECT OF COUPLED MODE SHAPES IN DENTAL IMPLANT

In this chapter, I will briefly provide some background about the modal analysis technique and its governing equations. Following that, I will present the theory of modal analysis for coupled and modified structures. Finally, the effect of coupled mode shapes in dental implant will be investigated both experimentally and numerically.

2.1 Introduction to modal analysis

Modal analysis is the process of determining the dynamic characteristics of a system in forms of natural frequencies, damping factors and mode shapes and using them to formulate a mathematical model for its dynamic behaviour. Modal testing is an experimental technique used to derive the modal model of a vibratory system. Theoretically, this technique is based on the relation between the vibration response at one location and excitation at the same or another location as a function of excitation frequency.

The hardware elements required in modal analysis measurements are exciters, transducers, and signal processing software. An exciter is a source of excitation used to provide a known or controlled input force to a structure. A *transducer* is a measurement device used to convert the mechanical motion of a structure into an electrical signal. A *processor* is needed to convert the time domain signal of the transducer to frequency domain. This arrangement is illustrated in Figure 2-1 [43].

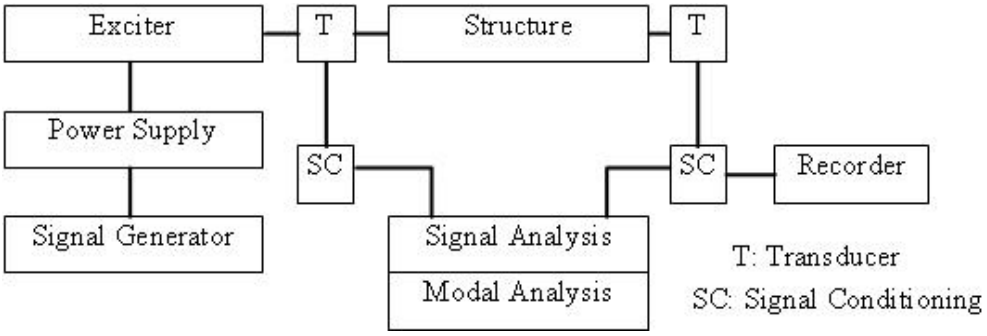

Figure 2-1: schematic of hardware used in performing a vibration test

2.2 Theoretical basis

2.2.1 SDOF system theory

Although very few practical structures could be realistically modelled by a single degree of freedom (SDOF) system, the properties of such a system are very important because more complex multi degree of freedom (MDOF) systems can be always represented approximately with a linear superposition of a number of SDOF systems. A representation of a typical SDOF system is shown in Figure 2-2.

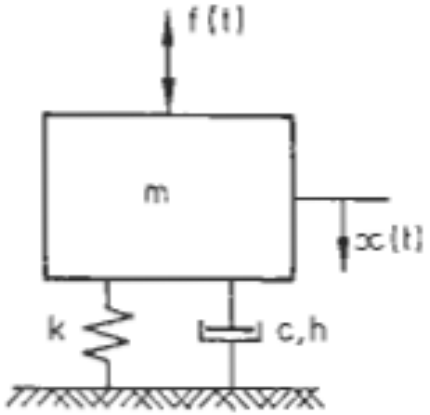

Figure 2-2: Single degree of freedom (SDOF) system

The equation of motion of the system is:

$$m\ddot{x} + c\dot{x} + kx = \mathbf{f(t)} \qquad \textbf{(2-1)}$$

For a general forcing function $f(t)=Fe^{i\omega t}$, the candidate solution can be written as $x(t)=Xe^{i\omega t}$, where ω is the frequency of excitation.

$$\dot{\boldsymbol{x}} = \boldsymbol{i\omega X e^{i\omega t}} \quad \textbf{(2-2)}$$

$$\ddot{\boldsymbol{x}} = \boldsymbol{-\omega^2 X e^{i\omega t}} \quad \textbf{(2-3)}$$

Substituting *f(t)*, $\dot{x}(t), \ddot{x}(t)$ and *x(t)* in (2-1) we have:

$$\boldsymbol{H(\omega) = \frac{1}{(k - m\omega^2) + i(\omega c)}} \quad \textbf{(2-4)}$$

Where $H(\omega) = X/F$ is called frequency response function (FRF) [44]. A non-dimensional version of the same expression is:

$$\boldsymbol{H(\omega) = \frac{1}{\left(1 - (\frac{\omega}{\omega_0})^2\right) + 2i\xi(\frac{\omega}{\omega_0})}} \quad \textbf{(2-5)}$$

Where ω_0 is the undamped natural frequency and ξ is the damping ratio.

$$\boldsymbol{\omega_0 = \sqrt{\frac{k}{m}}} \quad \textbf{(2-6)}$$

$$\boldsymbol{\xi = \frac{c}{c_0} = \frac{c}{2\sqrt{km}}} \quad \textbf{(2-7)}$$

2.2.2 MDOF systems with viscous damping

The general equation of motion for MDOF system with viscous damping is:

$$\boldsymbol{[M]\{\ddot{x}\} + [C]\{\dot{x}\} + [K]\{x\} = \{f\}} \quad \textbf{(2-8)}$$

Where [M], [C] and [K] are mass, damping and stiffness matrixes. To study MDOF systems, first the case where there is zero excitation in order to determine the natural modes of the system and to this end we assume a solution to the equation of motion, which has the form:

$$\mathbf{x(t)=u}\boldsymbol{e^{jwt}} \quad \textbf{(2-9)}$$

The receptance matrix is defined by:

$$\boldsymbol{\alpha(\omega) = (K - \omega^2 M + j\omega C)^{-1}} \quad \textbf{(2-10)}$$

The receptance matrix can be written as:

$$\boldsymbol{\alpha(\omega) = S^{-T} diag[\frac{1}{\omega_i^2 - \omega^2 + 2\xi_i\omega_i\omega_j}]S^{-1}} \quad \textbf{(2-11)}$$

Where *P* is the matrix of normalized eigenvectors of the matrix $M^{\frac{-1}{2}}KM^{\frac{-1}{2}}$ and $S = M^{\frac{1}{2}}P$.

2.2.3 The theory of coupled structures

In some cases, a complex structure that consists of an assembly of simpler components or substructures needs to be studied. To analyze coupled structures, the "impedance coupling method" or the "dynamic stiffness method" can be employed. This method is based on the frequency response properties of each individual structure and can provide the frequency response characteristics of the coupled structure [44]. The basic principle of coupled structure modal analysis as shown in figure 2-3 can be explained by two components A and B connected to each other from the side. Assuming that the dynamic of each component is considered quite independently as:

$$\boldsymbol{X_A = H_A F_A} \quad \textbf{(2-12)}$$

$$\boldsymbol{X_B = H_B F_B} \quad \textbf{(2-13)}$$

where H_A And H_B are defined as FRF of components A and B. Now, if the two components are connected and make system C, applying the conditions of compatibility and equilibrium, we have:

$$\boldsymbol{X_C = X_A = X_B} \quad \textbf{(2-14)}$$

$$\boldsymbol{F_C = F_A + F_B} \quad \textbf{(2-15)}$$

So that:

$$\boldsymbol{\frac{1}{H_C} = \frac{1}{H_A} + \frac{1}{H_B}} \quad \textbf{(2-16)}$$

This can also be written for more DOFs as:

$$\boldsymbol{[H_c]^{-1} = [H_A]^{-1} + [H_B]^{-1}} \quad \textbf{(2-17)}$$

This equation shows that in coupled structures the frequency response of the system can be extracted from the frequency response of its subsystems. In this chapter, the effect of coupled mode shapes of bone-implant structure on resonance frequency of implant is investigated. To simulate the effect of bone-implant integration, the implant is placed inside a chuck. The modal analysis of coupled implant/chuck is studied by both experimental and numerical approaches.

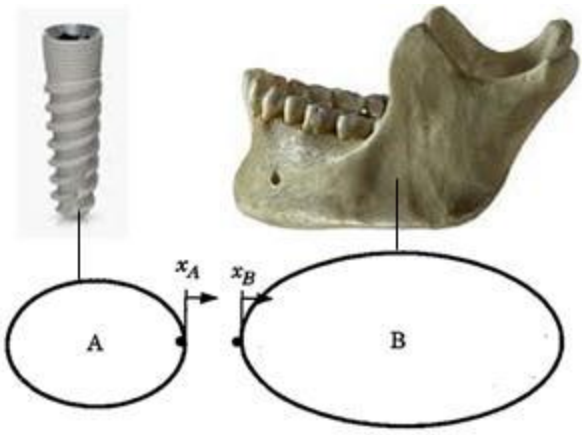

Figure 2-3: Basis of FRF coupling analysis

2.3 Experimental setup

The first step for investigating the effect of the coupled mode shapes is to do independent analysis on the RF of each substructure. To investigate the RF of implant, a 4.2×13 mm MIS endosseous implant is suspended by a rope (see Figure 2-4) and excited to oscillate by a transient force applied by an impulse force hammer (Dynapulse model 5800B2, Dytran instruments inc., USA). A non-contacting acoustic microphone (40BE repolarised free field microphone, G.R.A.S sound and vibration, Denmark) is used to record the vibration signal. Both the impulse force and the excited vibration response signal are transferred to a personal computer. The test is repeated for five times, and the average of five impact responses is used for each of the experiments (in total 25 tests). The signal analyser device Photon + is used to determine the frequency response function (FRF) of the implant. The maximum sharp value of FRF represents the resonance frequency of implant.

Figure 2-4: Test setup of implant modal analysis

Following that, the RF of implant is obtained when the same implant is fixed in a metal chuck stand under different holding intensity levels (see Figure 2-5). The implant is excited by an impact force applied with an impulse hammer installed as an inverted pendulum. A sliding joint is implemented in this setup in order to adjust hammer's position to hit the implant at the right location when the implant height is changed. The same non-contacting acoustic microphone is used to record the vibration signal. Both the impulse force and the induced vibration response signal are saved in the computer for frequency analysis. The tests repeated 10 times, and the final value of each test is obtained by averaging the 10 times triggering of the system (100 tests in total). Implant RF is measured at different free lengths. In this study, the term "free length" is referred as the length of implant left outside the jaw (chuck in these experiments). Twelve different free lengths are selected and excited by impulse hammer.

Figure 2-5: Test setup of implant/chuck modal analysis

2.4 FEM modelling of dental implant and coupled structure (implant/chuck)

The implant used in experimental set up is modelled in the SOLIDWORKS software (version 2009) (see Figure 2-6). To simplify the model, the thread portion in implant is neglected. The model is imported to ANSYS and then meshed (10,286 node / 6,159 elements) for resonance frequency analysis. Material properties of implant are considered homogenous and isotropic. The standard material property of the titanium dental implant is presented in Table 2-1. 3D 20-node structural solid element is used in the analysis. The boundary condition is set to free-free analysis (approximately similar to experiment condition of hanging the implant by a rope).

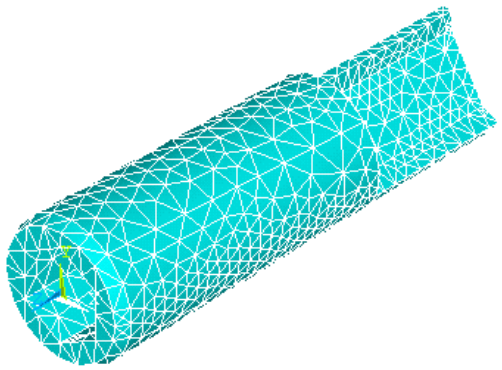

Figure 2-6: Model of implant meshed in ANSYS

Table 2-1: Material property of the implant

Young's modulus E (Mpa)	Poisson's ratio ϑ	Density ρ $(\frac{kg}{m^3})$
104.8	0.34	4430

The implant/chuck coupled structure shown in Figure 2-5 is also simulated in the SOLIDWORKS. The model is imported to ANSYS and then meshed for resonance frequency analysis (see Figure 2-7). The material property of implant is the same as listed in Table 2-1. 3D 20-node structural solid element is used in this analysis since it has three degree of freedom per node, has compatible displacement shapes and is well suited to model curved boundaries. The nodes on the back of the chuck are set to be fixed. The contact surfaces between implant and chuck are rigidly fixed in order to prevent the relative motion.

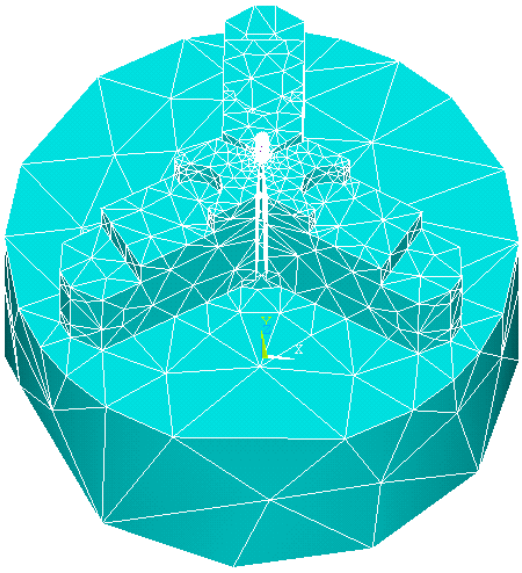

Figure 2-7: 3D model of implant/chuck meshed in ANSYS

2.5 Results and discussion

Experimental result of resonance frequency of implant indicates that the RF of implant suspended by soft rope happens at 73.7 KHz while analyzing the RF of implant in ANSYS simulation environment software shows that RF occurs at 73.8 KHz. Comparing experimental and numerical results disclose the reliably and accuracy of simulated implant model.

Figure 2-8 shows the experimental results for three different free lengths of implant, 9.4 mm, 8.88 mm and 7.7 mm when it is fixed by the metal chuck. From Figure 2-8, it can be seen that the peak of FRFs of the coupled system increases significantly from 11.1 KHz to 17.1 KHz. The experimental results indicate the sensitivity of RF of implant to the free length of implant.

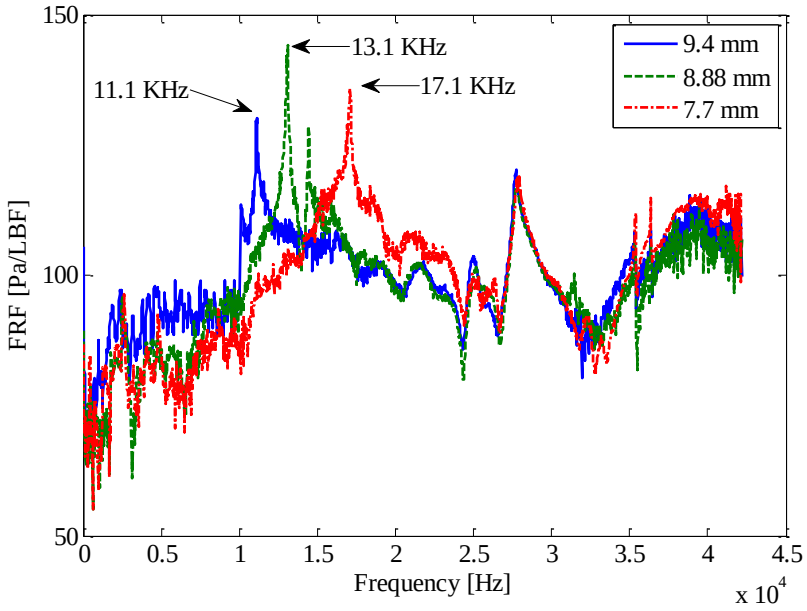

Figure 2-8: Experimental results of RF of implant for different free length

The experimental results of RF of implant when it is fixed by the metal chuck and the free length of implant is changed are tabulated in Table 2-2. While the free length varies from 9.4 mm to 4.29 mm, the resonance frequency changes from 11.1 KHz to 25.8 KHz. As it is shown in Figure 2-9, the correlations of resonance frequency values and the free lengths of implant is linear in the form of y= -2.871x+38.3. This finding agrees with the results of Haung *et al*. [34]. Their results showed that the natural frequency values decreased when boundary levels were reduces. They also found that there is a linear relation between RF of implant and the free length of implant.

Table 2-2: RF of dental implant under different chuck levels

	Free Length of implant (mm)											
	9.3	9.4	8.88	8.59	8.06	7.7	7.58	6.48	6.27	5.61	5.41	4.29
RF(KHz)	11.1	11.1	13.1	13.5	15.4	17.1	17.3	18.2	19.8	20.7	25.1	25.8

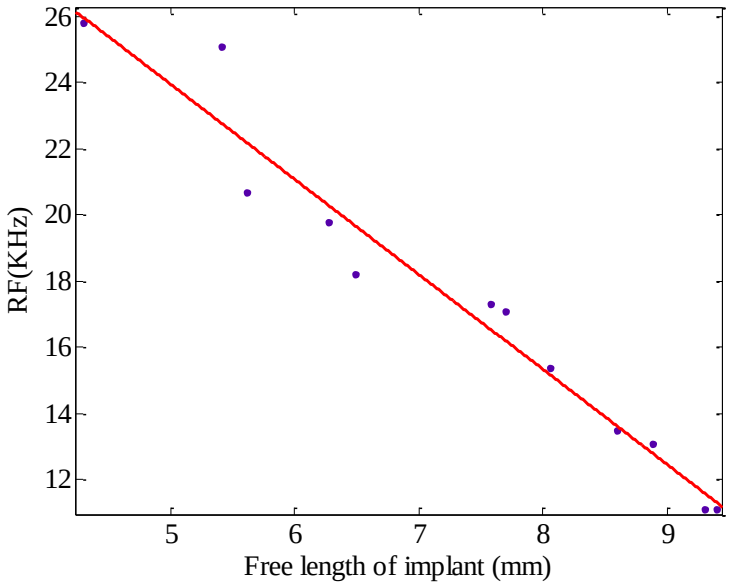

Figure 2-9: Plot of RF versus different free length of dental implant

Resonance frequencies of implant when it is fixed by metal chuck are also analyzed in ANSYS modal analysis simulation environment. Figure 2-10 shows the mode shapes of dental implant under different free lengths (9.4 mm and 8.88 mm). As it can be seen in this figure, the RFs of implant for the free lengths of 9.4 mm and 8.88 mm are 10.79 KHz and 13.68 KHz respectively. Comparing the analytical results and experimental results listed in Table 2-2, validates the FEM model.

The length of implant, suspended by soft rope, is 13 mm while different free length of implant is tested when it is fixed in metal chuck. There is an inverse relation between the free length of implant and the RF of it (it is discussed in chapter 3). Therefore, if the implant is shortened in order to apply same free lengths, the numerical and experimental results of RF of implant (suspended by soft rope) will be more than 73 KHz.

Since implant-chuck structure is a coupled structure, the mode shapes shown in the ANSYS post processing results include the mode shapes of the combination. However, to identify the mode shapes of the implant we should only consider those results where the implant motion is considerably higher that the chuck. In fact, that mode is the one captured by the measurement device and appears as the natural frequency of implant in our experimental results. Figure 2-10 shows that the RF of implant when the free length

is 9.4 mm is the twelfth mode shape of the system while the RF of implant when the free length is 8.88 mm is the eighteenth mode shape of system.

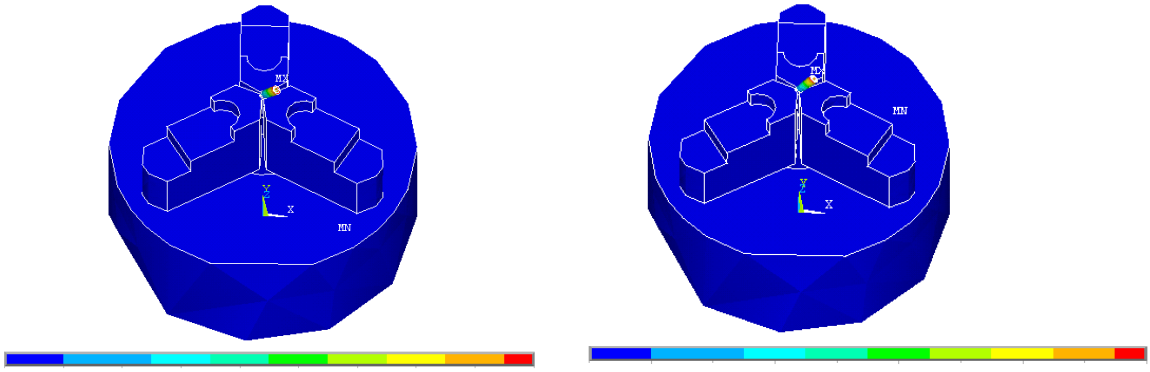

Free length: 9.4 mm, Frequency:10.79 KHz

Free length:8.88 mm, Frequency:13.68 KHz

Figure 2-10: The modes of implant/chuck system correspond to free length 9.44 mm and 8.88 mm

2.6 Conclusion

In conclusion, both experimental and numerical results show that the resonance frequency of a coupled implant/chuck is influenced by the material property of each individual units as well as the quality of their integration. Based on the results, it is concluded that the resonance frequencies of implant is still present but the values are changed in the coupled structure (placed inside the chuck). The RFs of implant extracted experimentally and numerically are 73 KHz, 73.7 KHz respectively. However, when the implant is fixed in chuck the RF of implant is dropped to 11.1 KHz (in case the free length of implant is 9.4 mm). Since each subsystem has unique FRF, it is expected that each coupled structure such as implant/bone should have unique RF characteristic.

3: A NUMERICAL APPROACH OF ESTIMATING DENTAL IMPLANT HEALING PROCESS USING RESONANCE FREQUENCY ANALYSIS (RFA)

Osseointegration is an important factor in specifying a series of criteria that identifies success or failure of an implant. Several reports pointed out that the status of healing process and early prediction can be achieved by studying the behavior of implants in surrounding tissue [45,46].

This chapter investigates the healing process of implants by monitoring the RF of the implant. In this study, the jaw-implant structure including titanium implant, cancellous bone and cortical bone is modeled in ANSYS modal simulation software. As the boundary condition of implant-bone interface changes during the healing process and because of the sensitivity of resonance frequency to boundary condition, it is expected that the resonance frequencies of implant changes as well. In this chapter the trend of frequency changes is analyzed to find the effect of bone-implant integration on natural frequency and predict the stage of healing process. For this purpose, the interface between the implant and jawbone is modeled by two rings, each to represent the cortical and cancellous bone. To simulate the process of integration, the mechanical properties of these rings are changed during healing process.

3.1 Materials and Methods

Healing process in dental implants is the time duration after the surgery and placement of implant in which the jawbone strongly bonds with implants. When dental implant is placed in the bone, healing process becomes apparent by the new bone cells formation at the implant site. The healing process increases continuously and it is completed when the implant-bone interface is fully integrated. Evaluation of the healing

process of implant cannot be accomplished easily. Assessing the effect of boundary condition on resonance frequency of the implant is a useful diagnosis method in early detection of healing process. As it is stated in chapter 2, the resonance frequency of structures, including dental implants, are related to the material properties as well as boundary conditions. The implant-bone integration is a time variant varying boundary condition. From the knowledge of mechanical vibration theory, resonance frequency of a cantilever beam that is fixed at one side and free to vibrate at the end can be stated as follows:

$$f = \beta \sqrt{\frac{EI}{\rho l^4}} \qquad \textbf{(3-1)}$$

Where l is the effective vibrating length of the beam, ρ is the vibration mass per unit until length, I is the moment of inertia, and β is a constant related to the boundary conditions [47]. According to (3-1) changing the boundary condition can directly affect the resonance frequency. In this study, the boundary conditions between implant and bone contact surface is changed to simulate the healing process while l, E, I and ρ are kept constant.

For investigating the effect of boundary condition on RF of implant and evaluating the healing process, a model of a jaw has been developed. In that model, cortical and cancellous bones, which are the two main parts of osseous tissue, are included. Two subparts, i.e. the cortical bone and cancellous bone are built similar to model used in a paper published by Wang et al. [40]. They simulated a real bone of bovine rib of a mature specimen. The bone-implant interfaces at the cortical and cancellous bone are constructed as rings. Since during the healing process the boundary condition between implant and bone changes continuously, Young's modulus of both cortical and cancellous rings were varied from 10% to 100 % of surrounding cortical and cancellous Young's modulus. To study the contribution of each of the cortical and cancellous bone structures in the RF of the bone/implant integration, the Young's modulus of one of them is fixed at 10% and the other one is varied from 10% to 100%. An implant (SEVEN system, MIS implant technologies ltd.) of 4.2 ×13 mm is used in our simulations. The implant is inserted into the bone and the simulations are conducted

for 7 and 8 mm implant free lengths. The model is analyzed in ANSYS to obtain the RF of dental implant (see Figure 3-1). To simplify the model and because of the negligible effect of threads on our desired analysis the FE model did not include the thread portion. The standard material property of implant is presented in Table 2-1. To evaluate the effect of mechanical properties of the interface on healing process, similar to [40] two different combinations of the bone's material properties are considered (Table 3-1). In addition, the cortical and cancellous bones are assumed to be homogenous and isotropic. The coinciding nodes of the contact surfaces between cortical and cancellous bone and rings are selected to be coincident, i.e. the displacement in all directions are all the same. 3D 20-node structural solid element is used in the analysis since it has three degree of freedom per node, has compatible displacement shapes and is well suited to model curved boundaries. The nodes of both lateral surfaces are fixed as boundary conditions.

Table 3-1: Different combinations of the bone's material properties

	Description	Young`s modulus E(Mpa)	Poisson's ratio ϑ	Density ρ (g/mm^3)
Combination 1	Cortical Bone	1.158×10^4	0.321	0.9301×10^{-3}
	Cancellous Bone	4.115×10^2	0.2636	3.5598×10^{-4}
Combination 2	Cortical Bone	3.474×10^4	0.421	2.7902×10^{-3}
	Cancellous Bone	12.345×10^2	0.3636	10.6792×10^{-4}

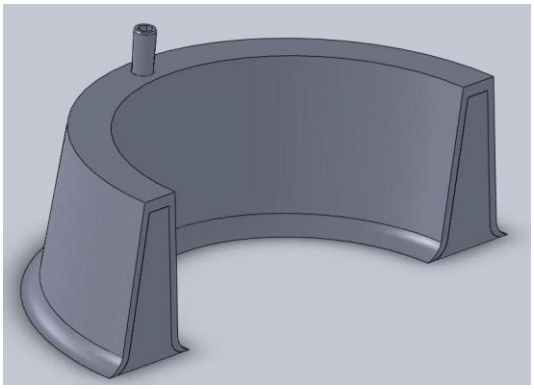

Figure 3-1 (A): The assembled model

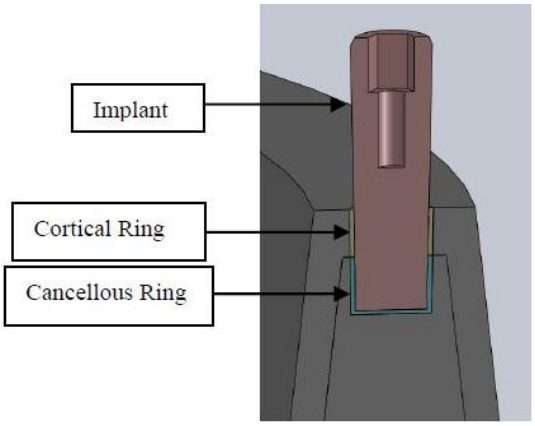

Figure 3-1 (B): Cross section of implant, cortical and Cancellous rings

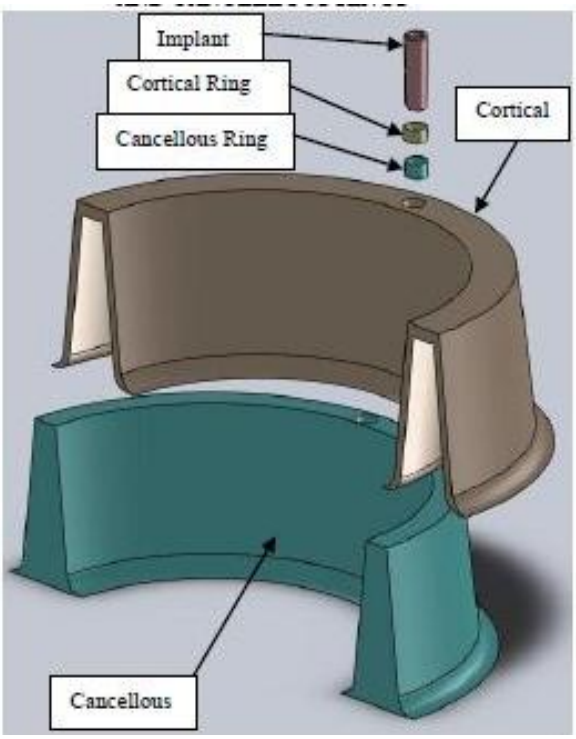

Figure 3-1 (C): The components of implant-bone structure model

3.2 Results

Figures 3-2 and 3-3 show the RF of the dental implant in three different case studies for each of the combinations. The first case (shown by solid line) indicates the situation when the Young's modulus of both implant-bone interfaces, i.e. cortical and

cancellous rings, were increased from 10% to 100%. The second case (shown by dash-dot) indicates the situation when the cancellous Young's modulus is fixed at 10% and the cortical Young's modulus is increased from 10% to 100%. Finally, the third case (shown by dash line) indicates the situation when the cortical Young's modulus is fixed at 10% and the cancellous Young's modulus is changed from 10% to 100%. In these figures, the free length of implant is 8 mm of implant. Figures 3-4 and 3-5 show the effect of free length of implant on RF (7 and 8mm). In these figures, the Young's modulus of both cortical and cancellous rings was increased from 10% to 100%. Since implant-bone structure is a coupled structure, the same approach as chapter 2 is used to find RF and we only selected the mode shape that the implant has its maximum deflection. Figure 3-6 shows the mode shapes and their maximum deformations (DMX) for the case of 8mm implant free length in combination 1 where the Young's modulus of both cortical and cancellous rings are in 10%. For that case, the last mode, i.e. No.19, is selected since it has the maximum amplitude of the implant deflection.

As it is shown in figures 3-2 to 3-5 the calculated RF of implant increases when the implant-bone integration completes. Considering figures 3-4 and 3-5, for the case that both cortical and cancellous Young's modulus varies from 10% to 100% of their surrounding bone material property, in combination 1 and for 8 mm implant free length, the RF increases from 19.3 KHz to 21.3 KHz, while in combination 2, it increased from 26.8 KHz to 28 KHz. For the case of 7 mm implant free length, the RF in combination 1 increases from 20.7 KHz to 22.6 KHz, while in combination 2 it increases from 31.4 KHz to 33.2 KHz. It can be concluded that during the healing process the RF increases and reaches a plateau when implant-bone is fully integrated.

Comparing results of Figure 3-4 and Figure3-5 shows that higher free length of implant results in lower RF. For example, in combination 1 in case of 7mm free length, for the 10% Young's modulus the RF is 20.7 while it is 19.3 in case of 8 mm.

All combinations show the trend of increasing the RF with changing boundary condition and reaching the plateau line after fully integration between bone and implant The figures 3-2 and 3-3 also indicate that the RF of implant for the case of fixed cancellous Young's modulus and cortical modulus increase from 10% to 100% is higher

than the case where the situation is reversed. The reason is that the Young's modulus of cortical is higher than the cancellous and thus it has a dominant effect.

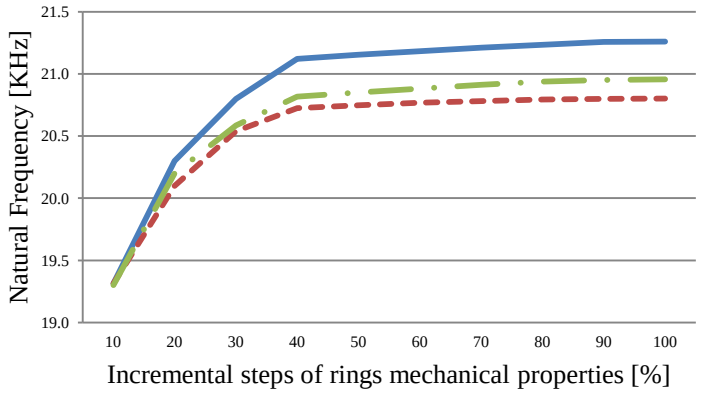

Figure 3-2: The resonance frequencies under different cortical and cancellous bone levels in combination 1 when 8 mm of implant is left out of bone

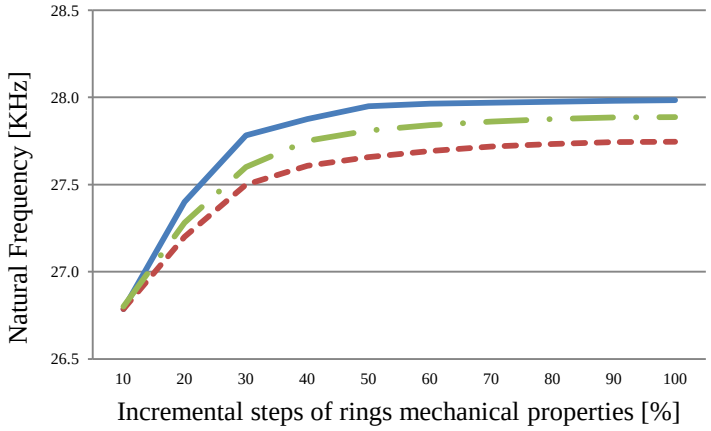

Figure 3-3: The resonance frequencies under different cortical and cancellous bone levels in combination 2 when 8 mm of implant is left out of bone

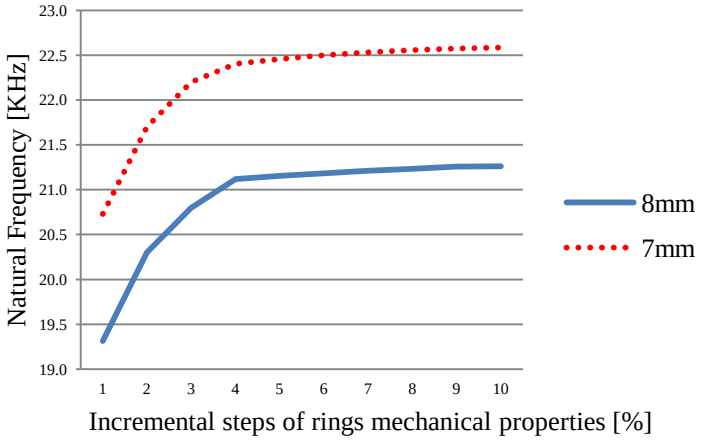

Figure 3-4: The resonance frequencies under different cortical and cancellous bone levels in combination 1 when 8 and 7 mm of implant is left out of bone

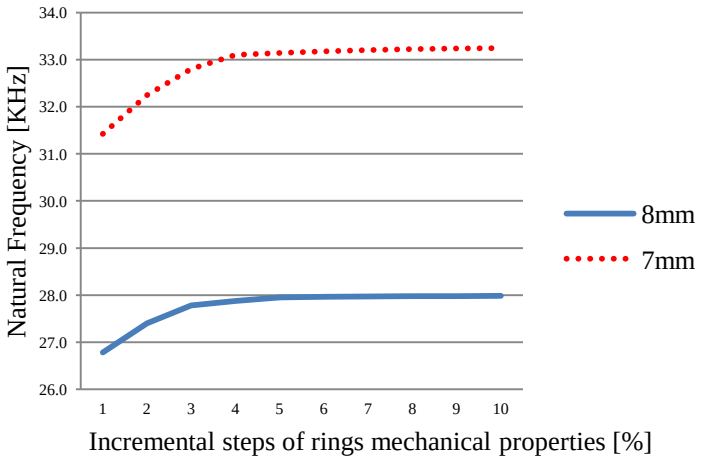

Figure 3-5: The resonance frequencies under different cortical and cancellous bone levels in combination 2 when 8 and 7 mm of implant is left out of bone

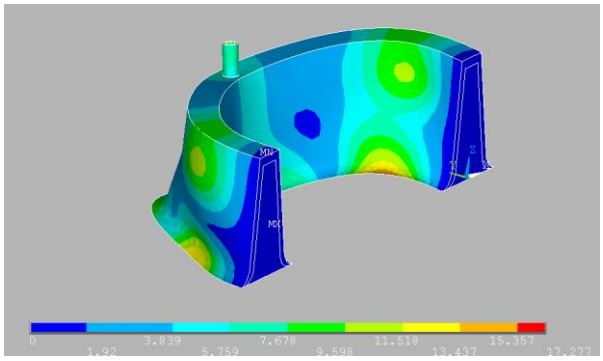

MODE#16, DMX=17.277

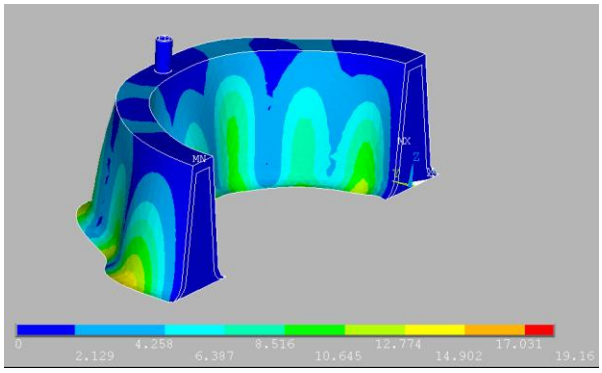

MODE#17, DMX=19.16

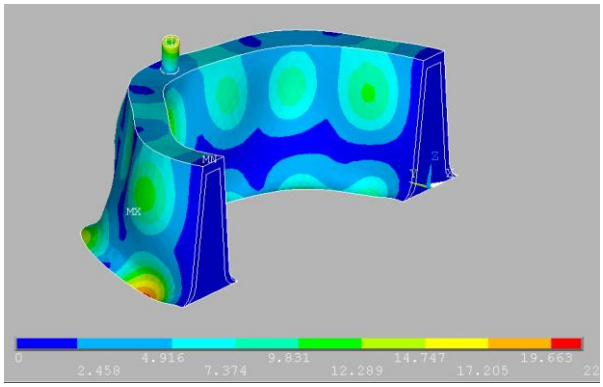

MODE#18, DMX=22.121

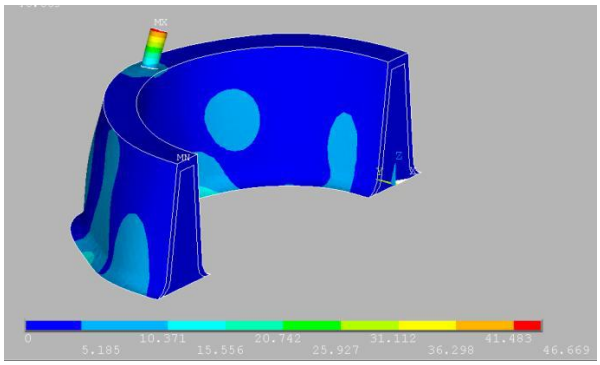

MODE#19, DMX=46.669

Figure 3-6 : The mode shapes of implant for 10% surrounding bone Young's modulus in case of 8mm of implant left out of the bone for combination

3.3 Conclusion

As it is shown in figures 3-2 to 3-5, for the two different combinations of bone's material properties, the RF of the implant increases when the implant-bone in more integrated and reaches to a plateau when the implant-bone interface is fully integrated. It can be concluded that monitoring the RF during the healing process can be used as a method to determine the stages of healing process. In practice, the precise value of the RF should be determined by *in vivo* experiments. The trend of increasing RF is in full agreement with the experimental results of paper [37]. Moreover, this analysis shows that the contribution of cortical bone in integration is more dominant than the cancellous since the cortical bone is a stronger bone than the cancellous.

4: THE EFFECT OF ENDOSSEOUS IMPLANT ANGULATION ON THE RESONANCE FREQUENCY OF IMPLANT

The use of dental implants in the rehabilitation of partially and completely edentulous patients is considered a predictable and successful treatment modality with favorable long-term survival rates [48-50]. To achieve a successful outcome, meticulous planning for surgical and prosthetic stages is mandatory. Complications, however, may occur in various stages leading to implant failure. Poor surgical techniques may result in poor implant placement in a compromised orientation in bone, which further complicates prosthetic rehabilitations. A poorly oriented implant may be jeopardized further by the lateral vector of the occlusal forces. In such situation, stress and strains concentrate primarily at the neck of the implant instead of the entire long axis, which can result in early bone loss and eventual implant failure. Implant angulation also can insert excessive strain on the crown superstructure. Eduardo *et al*. [51] reported that an increase in implant angulation resulted in an increase in stress intensities, independent of crown type. A poorly oriented implant also can affect the accuracy of the impression materials. Roberto *et al*. [52] found that implant angulation directly affected the accuracy of the impression by straining the impression materials. The use of computer-milled or laboratory fabricated surgical guides have greatly improved placement angulation; however, problems such as fabrication accuracy, placement limitations, and high cost limits their use. Since implant angulation errors can occur during implant placement surgery, there is a need for an objective method to evaluate and monitor the health of the tissue/implant interface.

RF is a parameter of a vibrating structure, which has been used as a non-invasive and objective method to monitor the short and long-term changes in implant stability [1,26,27]. Most of the RF data available in the literature obtained from the interface of

implants placed in an optimal orientation, and little data are available for RF of implants placed in compromised orientations.

The simulation method has the advantage of allowing independent control of each parameter in the FE models. This enables controlled and systematic evaluation of parameters such as implant orientation to the overall implant stability. Wang *et al.* [40] used RFA in finite element method to determine the identifiable stiffness range of interfacial tissue of dental implants. They found that when the Young's modulus of the interfacial tissue is less than 15Mpa, the RFs are significantly affected by the interfacial tissue but not the other parameters such as geometry, boundary constraint, and material property of the bone. RFA is used in this study because of its high sensitivity to boundary conditions and also non-invasiveness and non-destructiveness of this method.

This chapter aims to identify the relation between the RF of a screw-shaped endosseous dental implant in an optimal and compromised orientation (1-10 degree) using FEA simulation. MIMICS, a three dimensional (3D) modelling software is used and a 3D model of a pig mandible is constructed from computed tomography (CT) images. In addition, a cubical model is also created in MIMICS to investigate the parameters concerning the relation between RF changes and implant orientation in a simplified environment. Our analysis showed that the ratio of cortical to cancellous bone contacting the implant is the main factor in determining the relation of implant orientation and the RF of the implant.

4.1 Material and methods

In this study, FEM is used to perform FEA in two models, a partial pig mandible and a simplified cubical epoxy resin block.

4.1.1 Pig mandible model

A mandible of domestic young adult pig is obtained from the slaugher house (Britco Pork Inc.) and a 3.75×13 mm MIS endosseous implant is placed at the edentulous space between 1st and 2nd premolars. MIS surgical protocol is followed to obtain primary stability in bone. A 13 mm titanium MIS abutment is torqued to the implant body at 32

N/Cm^2. The mandible is later block sectioned at the premolar areas to include the implant and adjacent teeth (Figure 4-1a).X-ray computed tomography of the sectioned mandible is performed using a Kodak Cone Beam Computed Tomography (CBCT). Figure 4-1b shows the transverse plane of CT image slice of the sectioned pig mandible. DICOM (Digital Imaging and Communications in Medicine) x-ray images were individually imported into MIMICS (version 14.12) to create an accurate, 3D model of the sectioned mandible, teeth and implant. The model is later imported into FEA software, ANSYS (version 12.1) for simulation RF analyses. In FEA, a physical system, such as the pig mandible model is converted into a number of discrete elements and the properties of each element is assigned from the bank of standard reference data.

Tissues and implant were identified in MIMICS from individual DICOM images using a default threshold technique. A radiologist expert also confirmed and corrected the threshold criteria for the identifiable structures. These structures included cancelous and cortical bone, enamel, dentine, soft tissue, and implant. Cementum and dental pulp were excluded because of their relatively low volume and thus minor contribution in the analysis.

Figures 4-1c shows one of CT image slices of the segment of pig mandible in which the cortical, cancellous, enamel and dentine are shown. Figure 4-1d shows the 3D model of the sectioned pig mandible, teeth and implant.

The CBCT images of pig mandible is meshed in MIMICS (51300 nodes / 28967 elements) and imported into ANSYS and a 3D 10-Node tetrahedral structural solid element is used for the RF analysis. The element is defined by ten nodes having three dimensional motion at each node, which is well suited to model irregular meshes. The coincidental nodes of the same mutual contact surfaces are rigidly fixed in order to prevent relative motion, i.e. the displacements in x-, y- and z-directions are all set to be the same for the same coinciding nodes. The material properties of cortical/cancellous bone, enamel, dentine, and dental implant are listed in Table 4-1 [53], and the properties of different elements of this model are all assumed homogeneous and isotropic.

Implant is placed parallel to the long axis of the 2^{nd} premolar through the middle of the crestal bone. The effect of implant orientation on the RF of implant is analysed when the centre of mass of the implant is rotated from 1º to 10º in 1º increment about the

y-axis (see Figure 4-2). In addition, the implant is subsequently extruded in positive z-axis direction in increments of 0.5 mm and 1 mm and RF analyses were repeated. This simulation is conducted to investigate the effect of the implant free length (the length of implant out of the bone) on RF.

Table 4-1: Material properties of the 3D segment of pig mandible

	Young's modulus E (Gpa)	Poisson's ratio ϑ	Density ρ $(\frac{kg}{m^3})$
Cortical bone	14	0.3	1300
Cancellous bone	0.49	0.3	1300
Dental implant	104.8	0.34	4430
Enamel	75	0.33	2970
Dentine	15	0.31	2140

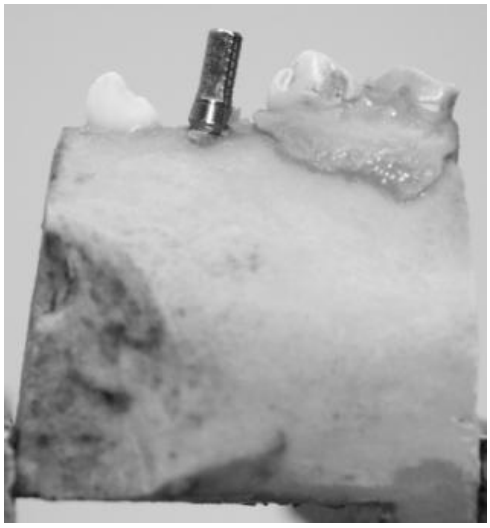

(a)

(b)

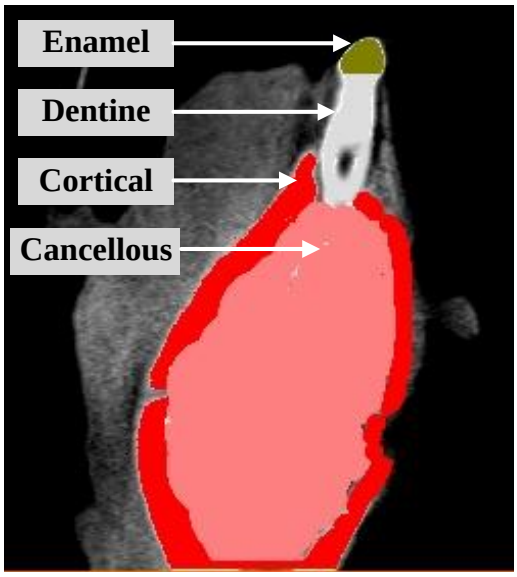

(c)

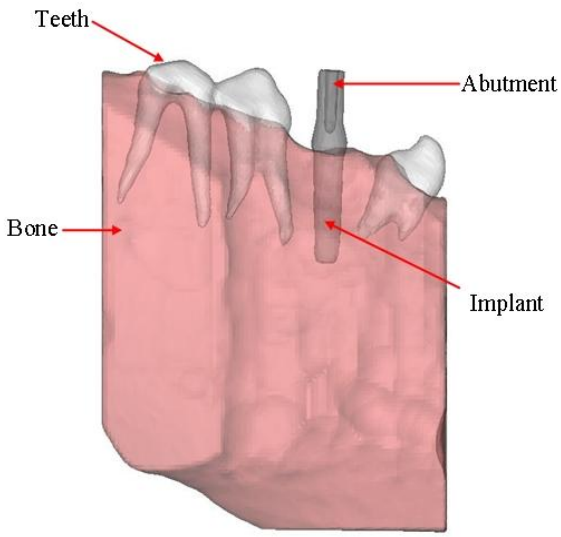

(d)

Figure 4-1: (a) a section of pig mandible. (b) Transveres plane of one of CT image slices of sectioned pig mandible (c) A CT image slice in which the cortical, cancellous bone, enamel and dentine are shown (d) 3D model of pig mandible showing bone, teeth, implant and abutment

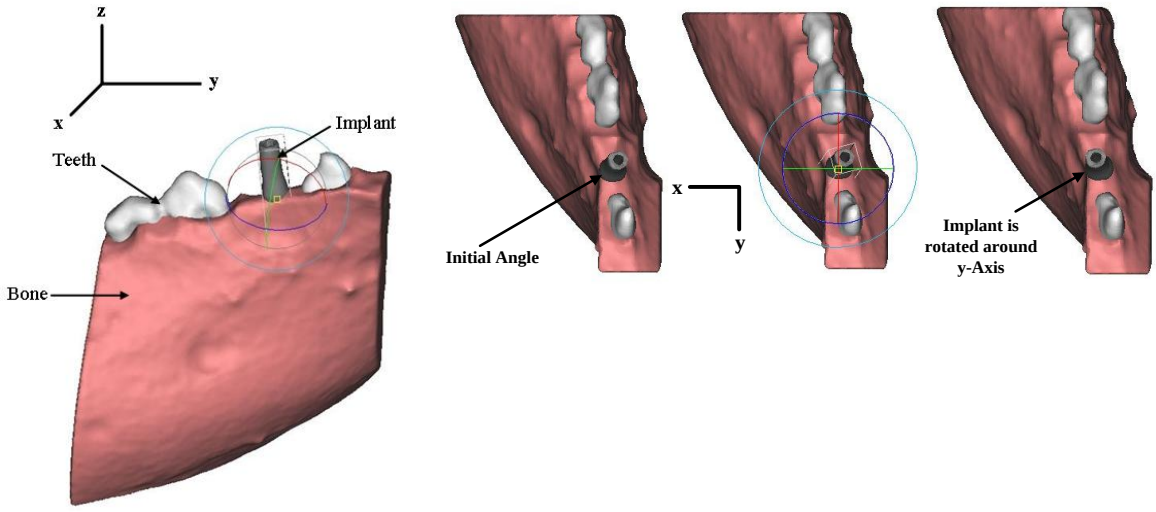

Figure 4-2: The centre of mass of implant is rotated about y-axis from 1º to 10º in 1º increments.

4.1.2 Simplified Epoxy cubical model A & B

Simplified models (A & B) are designed to reduce the potential interference of heterogenousity of adjacent structures in RF analyses. Epoxy resin is poured into a polyvinyl silicon mold of the following dimensions (31 mm× 31 mm×25 mm). MIS SEVEN dental implant (a type of implant) is fully buried in the epoxy at the centre of the mold and allowed to cure for 2 days. Then a 13 mm MIS abutment is screw torqued (30 N/cm^2) to the implant. The simplified model block is then CT scanned using the Kodak Cone Beam Computed Tomography. DICOM CT images were imported in MIMICS to create 3D model. The models is meshed and imported to ANSYS for RF analysis. The same meshing element used for the sectioned pig mandible is used in the simplified models. The Epoxy resin surrounding the implant in model A is given either cancellous or cortical bone material properties (see Figure 4-3a). In Model B, the bulk of the epoxy resin is assigned cancellous bone properties, and the 5 mm thick surface layer of epoxy is assigned cortical bone properties (see Figure 4-3b).

Similar to the pig jaw model, the effect of implant orientation on its RF is analyzed when its center of mass is rotated from 1º to 10º in 1º increment about the y-axis. As the implant rotates, it is expected that two parameters are changed, the implant angle and the contact area with the bone. The effect of each parameter is investigated in

model A. To isolate the effect of each parameter on the RF, the FEA is performed while the impact of the second parameter is maintained constant. For example, the contact area with the implant is maintained constant by altering free length of the implant while the effect of the rotation is investigated. The parameter of h shown in Figure 4-4 is defined as the distance between the reference point (RP) and a fixed reference coordinate system (RCS). The RCS is fixed during the implant rotation. The RP is the point of intersecting horizontal contact line of implant and bone.

To study the effect of contact area on the relationship between implant orientation angle and the RF, the implant angle in the bone is maintained constant while the contact area of implant and bone is altered. This is achieved by slicing the lower threads of the implant. Three different situations is investigated when 0.54 mm, 1 mm and 1.53 mm of the lower threads of implant were omitted.

Because of considerable difference in material properties of cortical and cancellous bone (0.49Mpa vs. 14Mpa) in model B, the ratio of contact surface between cortical bone and implant to contact surface between cancellous bone and implant is considered as a potential influencing parameter affecting the RF of implant in different orientation. Therefore, a dimensionless quantity is introduced as Cortical to Cancellous Bone Ratio (CCBR) to investigate the effects of changing CCBR in RF of implants in different orientation angle.

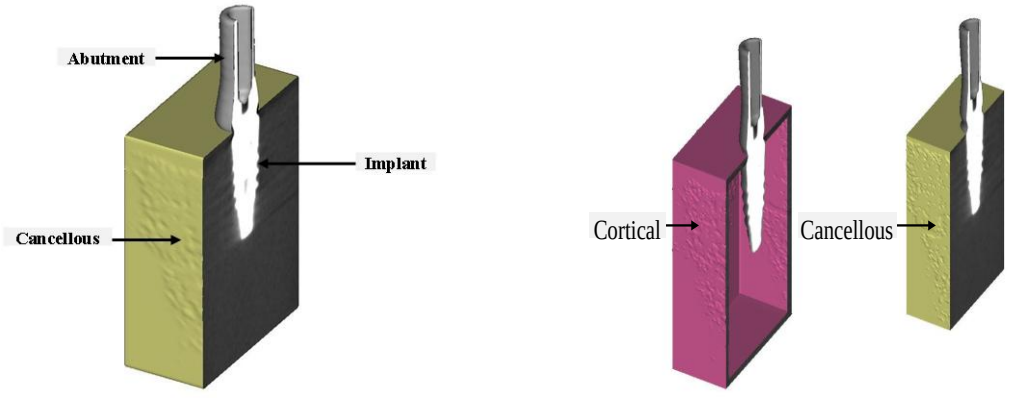

(a) Model A **(b) Model B**

Figure 4-3: simplified bone models (model A & B)

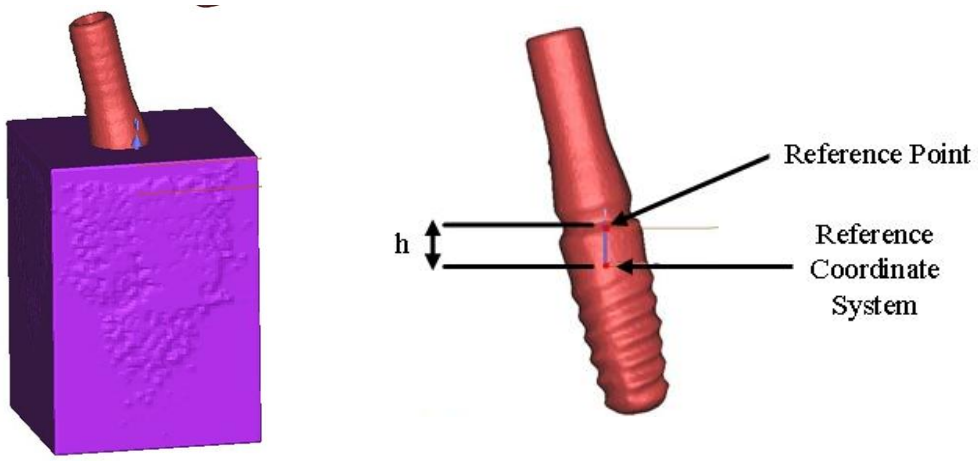

Figure 4-4: The parameter h defined as the distance between reference point and reference coordinate system

4.2 Results

4.2.1 Pig mandible model

The method of transferring DICOM CT-images into MIMICS resulted in the reconstruction of an accurate model representing a true virtual simulation of the implant in the bone. The ANSYS engineering software further allowed accurate FEA analyses of RF in the simulated model. The results of RF of implant for different implant orientations are tabulated in Table 4-3a. From Table 4-3a, it can be seen that the resonance frequencies of implant decrease considerably when the implant is moved in positive z-direction. For instance, the resonance frequencies of the implant when it is fully buried and 1 mm moved in the positive z direction, both rotated 1º about y axis, are 12.17 KHz and 9.69 KHz respectively. The results indicate that the implant free length affect the resonance frequency of implant. This observation agrees with the results of Huang *et al.* [34]. They found that the natural frequency of implant decreased when the boundary level (clamping level) were reduced.

Table 4-3a exhibits a jump in resonance frequency of implant. When the implant is buried in the bone, the jump happens from 6º to 7º and it occurs from 5º to 6º when the implant is moved 0.5 mm and 1 mm in positive z-direction. The reason of this jump is

investigated by exhibiting the results of parameters affecting the relation between implant orientation and RF of implant.

4.2.2 Simplified Epoxy cubical model A & B

The resonance frequencies of implant in model A are obtained and listed in Table 4-2b. The median of RF of implant when the cancellous bone material properties compose the model A is 9.83 KHz while it is 24.94 KHz when the epoxy resin surrounding the implant is given cortical bone material properties. The results indicate that in case only cortical or cancellous bone composes the bone, the effect of material properties on the relation between RF of implant and implant orientation is negligible.

The RFs of implant when the contact areas of implant and bone are fixed for all angle variations are listed in Table 4-2c.

The RF of implant in Table 4-2c is higher than those corresponding in Table 4-2b. This may be related to the effect of rotation but further investigation declares that these differences in RF are directly related to parameter h. In order to investigate the effect of rotation, the contact area is fixed and the free length of implant is decreased, consequently the parameter h is decreased. For instance, the h is 2.83 mm for 1 degree rotation while it is 2.08 mm for 10 degree rotation. The RF of implant is increased when the free length of implant is decreased. The result is coincident with the result of Table 3a. In conclusion, no definite relation is found in investigating of the effect of rotation between implant orientation and the RF of implant.

The RFs of implant in case the effect of contact area is studied are listed in Table 4-2d. The results indicate that the effect of contact area on RF of implant is negligible

In Summary, the results indicate that material properties, rotation and contact area have not significant contribution on the relation between implant orientation and the RF in model A.

The resonance frequencies of implant in model B are listed in Table 4-2e. To find the relationship between implant orientation and the resonance frequency of implant, the curves of the RF and CCBR values with respect to angles are scaled and depicted in the Figure 4-5.

From the Figure 4-5, it can be seen that there is a close relationship between the resonance frequency of implant and CCBR values. The CCBR values are also obtained in pig mandible model. Because of the complexity of the pig mandible model, the CCBR values are acquired approximately. The CCBR values are listed in Table 4-3b for the case of implant is moved 0.5 mm in positive z-direction.

Table 4-2: Results of model A & B

a- CCBR values in model B

	Rotating angle (degree)									
	1	2	3	4	5	6	7	8	9	10
CCBR	0.083	0.084	0.083	0.084	0.084	0.083	0.086	0.086	0.088	0.085

b- The RF of implant corresponding to model A : KHz

RF when Cortical bone compose A	24.86	24.94	24.91	24.95	24.94	24.93	25.05	25.06	25.09	25.09
RF when Cancellous bone compose A	9.85	9.85	9.84	9.84	9.83	9.82	9.83	9.82	9.81	9.8

c- The RF of implant corresponding to the effect of rotation in model A : KHz

RF when Cancellous bone compose A	9.85	9.85	9.87	9.92	10	10.01	10.08	10.11	10.19	10.29

e- The resonance frequencies corresponding to model B: KHz

RF	24.9	24.93	24.9	24.94	24.92	24.89	24.97	24.97	25.02	24.94

d- The resonance frequencies corresponding to the effect of contact area in model A: KHz

	The cutting length of lower thread part of implant (mm)		
	0.54	1	1.53
RF	10	10	9.97

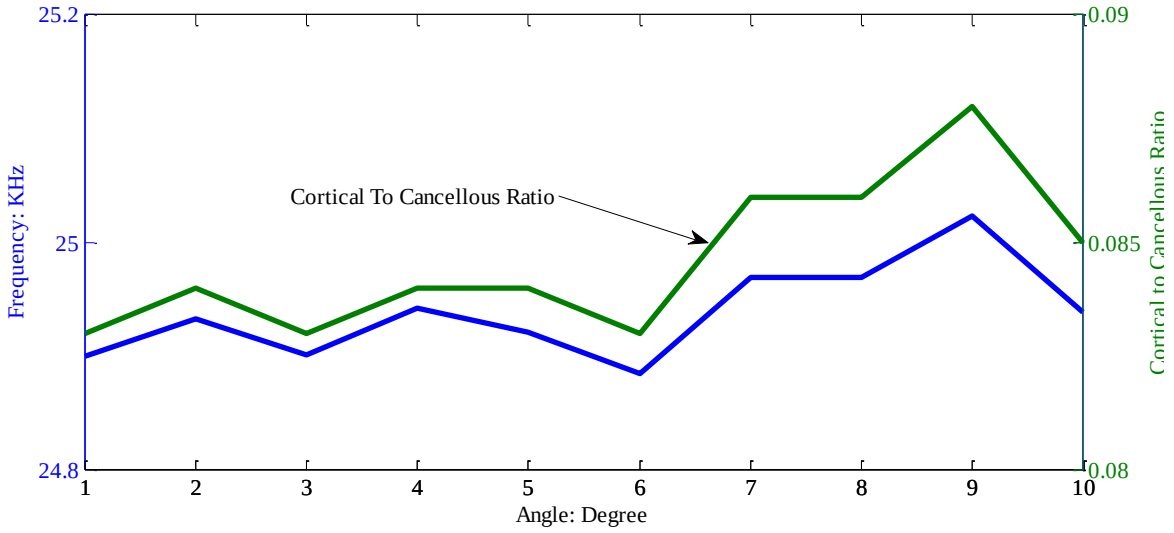

Figure 4-5: The RF and CCBR values with respect to angles in model B

For better realization of the relationship between implant orientation and the resonance frequency of implant, the curves of the RF of implant and CCBR values with respect to angles are scaled and depicted in the same graph, Figure 4-6. It can be seen from Figure 4-5 and 4-6 that there is a strong relationship between the resonance frequency of implant and the CCBR values. RF fluctuation following altering implant orientation is strongly influenced by the contacting cortical to cancellous bone ratio (CCBR) at the implant interface. This finding explains the jumps in RF in Table 4-3a properly.

Figure 4-7 exhibits the behaviour of RF of implant versus CCBR for different implant orientations. The central mark is the median, the edges of the box are the 25th and 75th percentile, the top mark is maximum value and the bottom mark is the minimum value. As it can be seen, these statistical marks are increased when the CCBR is increased and reached a plateau. It shows that the RF following altering implant orientation is directly affected by CCBR value.

Table 4-3: Results of pig mandible

a. The RF of implant corresponding to the segment of pig mandible: KHz

	Rotating angle (degree)									
	1	2	3	4	5	6	7	8	9	10
RF when Implant is buried in the bone	12.18	12.21	12.02	11.98	12.03	12.09	12.72	12.98	12.87	12.94
RF when Implant is moved 0.5 mm in positive z-direction	9.86	9.88	9.76	9.7	9.81	10.07	9.85	9.8	9.84	9.6
RF when Implant is moved 1mm in positive z-direction	9.69	9.52	9.58	9.53	9.52	9.88	9.71	9.62	9.49	9.5

b. CCBR in segment pig mandible when the implant is moved 0.5mm in positive z-direction

CCBR	53.4	53.5	52.6	52.2	52.9	54.8	54	53.6	54	53.1

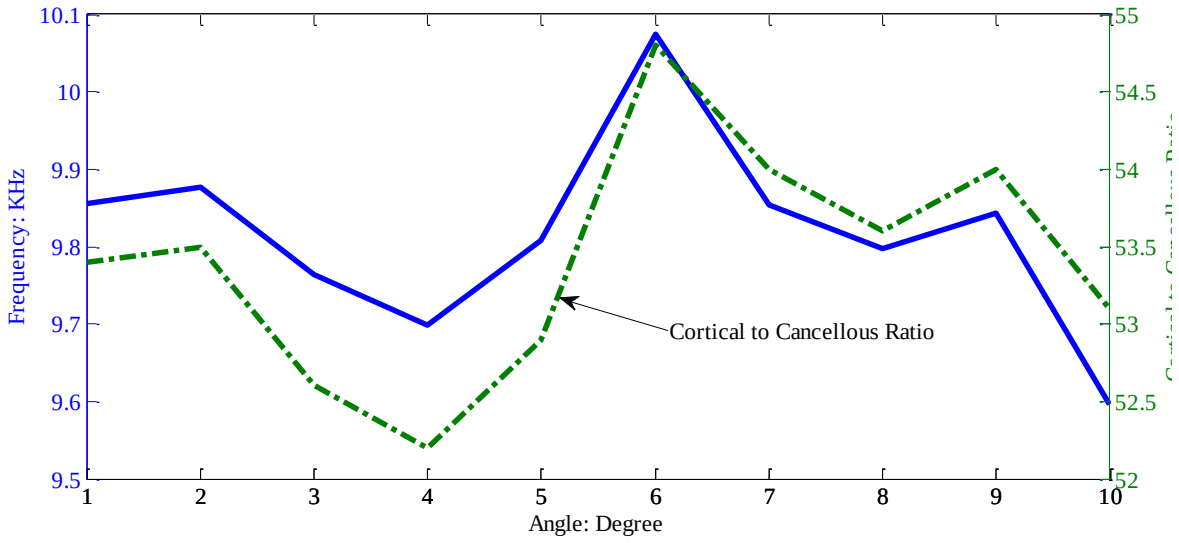

Figure 4-6: The RF and CCBR values with respect to angles in pig mandible model

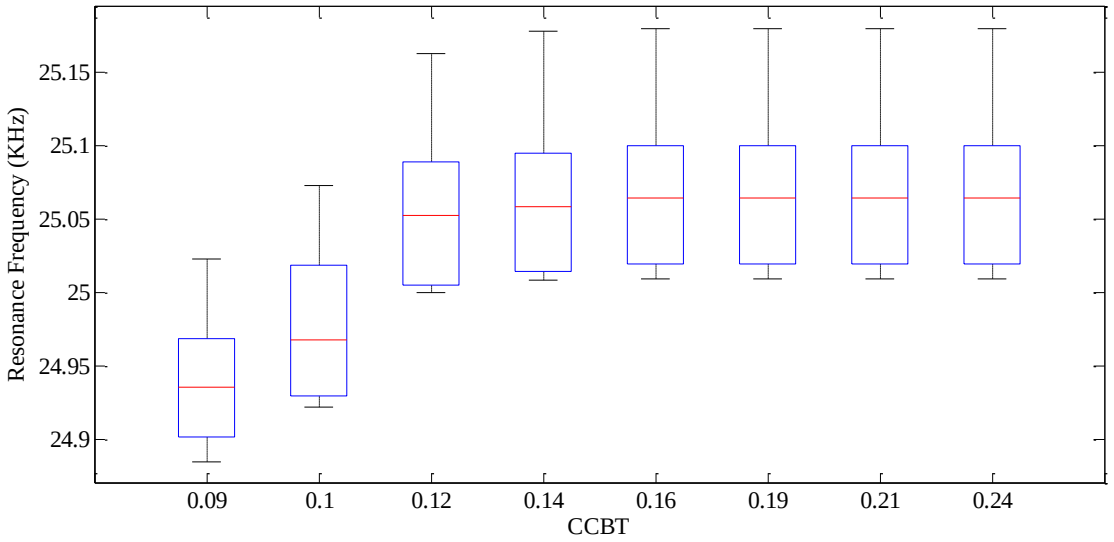

Figure 4-7: The behaviour of RF of implant versus CCBR for different implant orientations

4.3 DISCUSSION

To detect implant stability, various diagnostic analyses have been employed including percussion test, standardized radiographs, cutting torque resistant analysis, reverse torque test, and resonance frequency analysis (RFA) [8]. RFA method has recently became popular because it is a noninvasive diagnosis method and the most accurate technique. Atsumi *et al*. [8] classified the clinical applications of RFA including (1) a relation between exposed implant length and resonace frequency or ISQ (Implant Stability Quotient) values ;(2) differential interarch and intera-arch ISQ values for implants in various locations (3) prognostic criteria for long term implant sucess; and (4) diagnostic criteria for implant stability [54,30]. No study has been conducted to determine the relation between the resonance frequency of implant and implant orientation.

In this study, by using FEA simulation, the relation between the RF of implant in an optimal and comporomised orienation is identified. A three dimensional modelling software is used and a 3D model of a pig mandible is constructed. Moreover, a simplified epoxy cubical model is carried out to reduce the potential interference of heterogenousity of adjucent structure in RF analyses. The effects of material properties, rotation and contact area on the relation between RF of implant and implant orientation are investigated in model A. The results demonstrates that in case only cortical or cancellous

bone composes the bone, the effect of thsese paramaters are insignificant. Astrong relation between implant orientation and RF of implant is found by depicting the curves of the RF of implant and CCBR values with respect to angles (Figure 4-5 and 4-6). This finding is also supported by the investigating the results of Figure 4-7 showing that the RF of implant is increased in higher values of CCBR.

The RFs in model B where there is a thin layer of cortical bone is likely similar to the RF values in model A when the entire contacting area is given by cortical bone. The material properties of cortical bone are higher than cancellous bone material properties (comparing 14 Gpa to 0.49 Gpa), so when the implant is interfaced with both cortical and cancellous bone, even there is a thin layer of cortical bone, the RF of implant is mainly influenced by hard tissue, not soft tissue.

In clinical applications, different individuals have different CCBR values. Therefore, it is expected that each individual has a unique amount of RF of implant for a specific orientation. As it can be realized in Figure 4-7, for a specific implant orientation, there is a unique value for RF of implant depends on the CCBR value.

Figure 4-8 shows the mode shapes and their maximum deformations (DMX) for the case of implant is buried in the bone and it rotates 1 degree around y-axis. The last mode, No.18, is selected since the maximum amplitude of vibration happens at the implant.

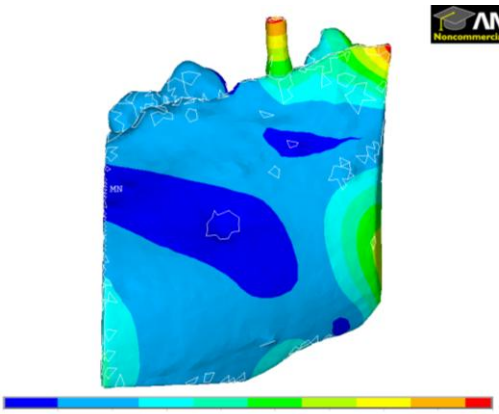

Mode #: 11, Frequency: 7348 Hz, DMX=26

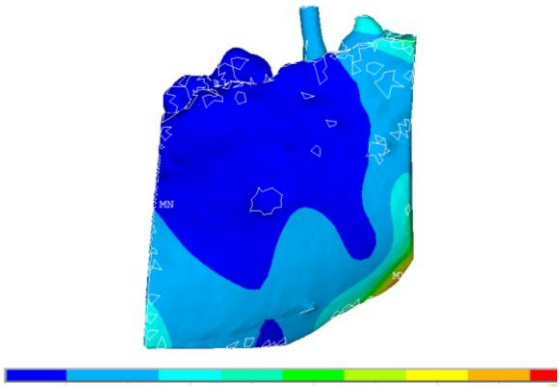

Mode #: 12, Frequency: 9091 Hz, DMX=34

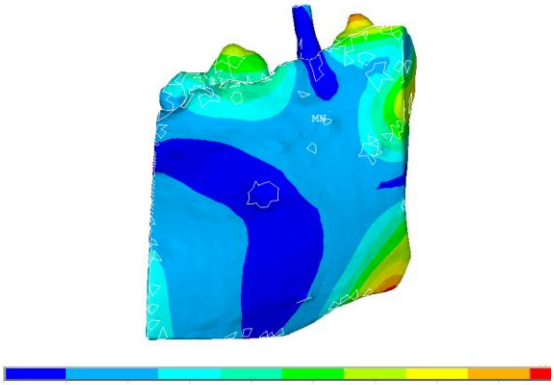

Mode #: 13, Frequency: 9397 Hz, DMX=23

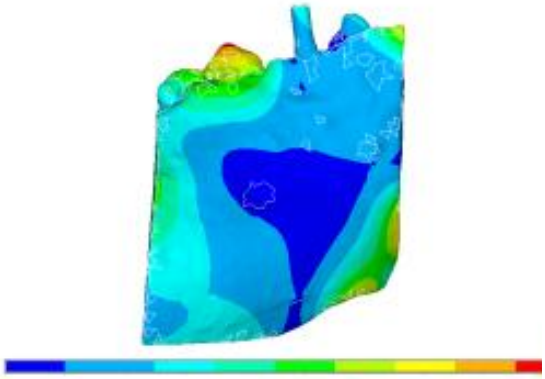

Mode #: 14, Frequency: 9740 Hz, DMX=22

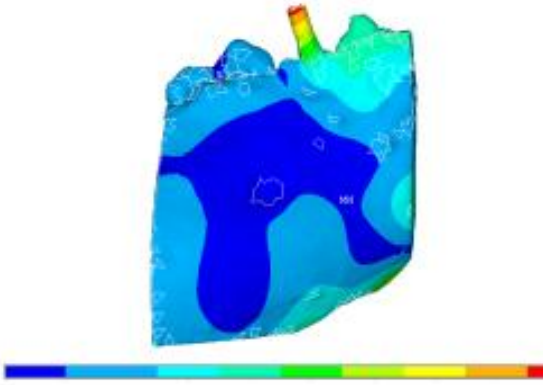

Mode #: 15, Frequency: 10349 Hz, DMX=27

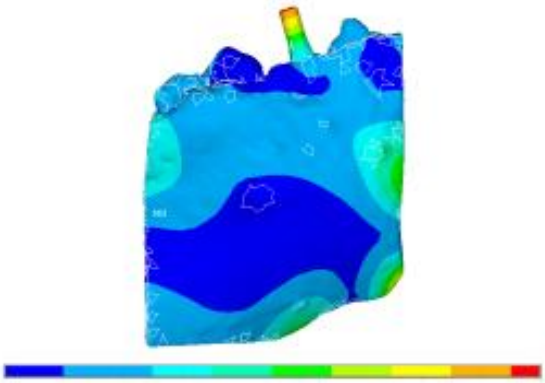

Mode #: 16, Frequency: 10789 Hz, DMX=31

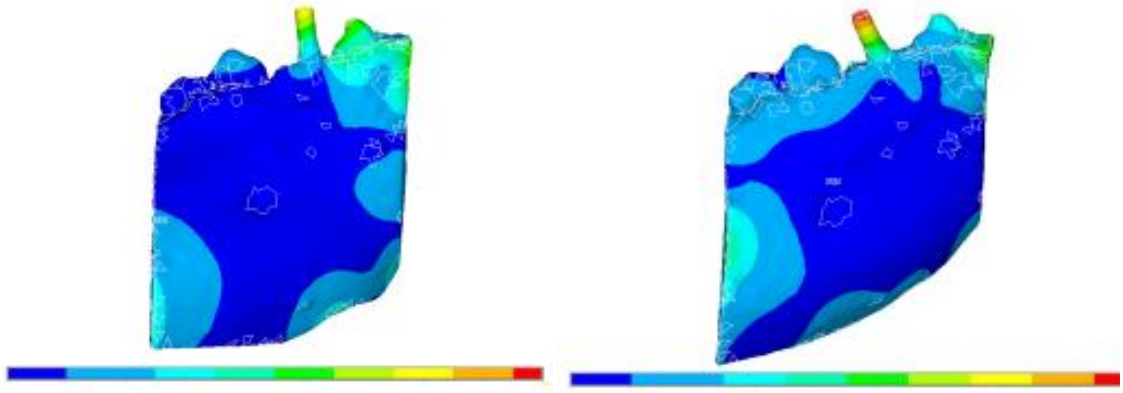

Mode #: 17, Frequency: 11739 Hz, DMX=41 **Mode #: 18, Frequency: 12175 Hz, DMX=42**

Figure 4-8: The mode shapes of implant for the case of implant is buried in the bone and it is rotates 1 degree around y-axis

4.4 CONCLUSION

In this study, we used the RFA method to determine the relation between implant orientation and the resonance frequency of implant. A 3D modelling software is used to construct a 3D model of a pig mandible from computed tomography images. Simplified models (A & B) were also carried out to investigate the parameters concerning the relation between RF changes and implant orienation in a simplified environment. It is found that material properties, rotation, and contact area have minimum contribution to the relation between implant orientation and RF of implant. We also found that the resonance frequency of implant is changed and strongly influenced by the cortical to cancellous bone ratio (CCBR) in interfacing areas of implant and bone. Based on the results, the higher RF of implant happens at higher values of CCBR independent of angle. In addition, by extruding the implant in positive z-axis in pig mandible model, we found that the free length of implant influences the resonance frequency of implant. Increasing the free length of implant resulted in decreasing the RF of implant.

In conclusion, the computational results demonstrate the capability of RFA method in determining the relation between implant orientation and resonance frequency of implant.

5: THE EFFECT OF SOFT TISSUE SURROUNDING THE IMPLANT ON THE RESONANCE FREQUENCY OF IMPLANT

As it is mentioned in chapter 1 implant stability depends on the successful osseointegration. It is also mentioned in chapter 1 that the surrounding soft tissue plays an important role in osseointegration of implant. When the implant is placed in the bone, soft tissue forms in the contact surfaces between implant and bone. The regenerated soft tissue at the implant/bone interface changes gradually to hard tissue during the process of osseointegration. Failure cases happen when implant bone interface is not fully osseointegrated or the hardened soft tissue at the interface fails (soft tissue forms at the failure locations). Wang *et al*. [40] classified the tissue into three phases considering different statuses of Osseointegration in the primary stability: the early healing phase which is the first phase after implantation in which the callus (a new growth of osseous matter at the ends of a fractured bone, serving to unite them) is composed of granulation (fibrous connective tissue), the middle phase in which the fibrous tissue is predicted in callus and the final tissue in which the cartilage (flexible connective tissue) is generated [55]. Since the mechanical properties of all of these phases are softer than their surrounding cortical and cancellous bone, hypothetically it is estimated that there is a relation between the resonance frequency of implant and the soft tissue in the primary stability. Wang et al [40] checked the relationships between the status of tissue and the first/second resonance frequencies of the implant-tissue-bone system and found the identifiable range of interfacial tissue of dental implants by means of resonance frequency analysis.

This study aims to identify the effect of soft tissue surrounding the implant on RF of implant using FEA simulation. MIMICS, a three dimensional (3D) modelling software is used and a 3D model of a pig mandible is constructed from computed tomography (CT)

images. A vigorous parametric study is conducted to disclose the relation between RF of implant and the surrounding soft tissue. Our analysis showed that the resonance frequency of implant is significantly affected by soft tissue when it is formed in cortical bone. In addition, the location and the size of soft tissue are two factors that influence the RF of dental implant.

5.1 Materials and methods

5.1.1 The modelling of the pig jaw and soft tissue

A mandible of domestic young adult pig is obtained from a slaughter house and a Ø3.75 X 13 mm MIS endosseous implant is placed at the edentulous space between 1st and 2nd premolars by a dental implant surgion. MIS surgical protucole is followed to place the implant so that primary stability of the implant is established in the bone. A 13 mm titanium abutment is torqued to the implant body at 32N/Cm^2. Due to the size limitation of CT machine, the mandible is later block-sectioned at the premolar areas. This section includes the implant, shown in Figure 4-1a. X-ray imaging of the sectioned mandible is performed using a Kodak Cone Beam Computed Tomography unit (CBCT). DICOM x-ray images were imported into MIMICS (version 14.12) to create an accurate, 3D model of the mandible, teeth and implant. To simplify the model and because of the negligible affect of threads on our desired analysis the 3D dental implant model does not include the thread portion. The model is later imported into finite element software, ANSYS (version 12.1) for investigating RF analyses. In finite element analysis (FEA), a physical system, such as the pig mandible model is converted into a number of discrete elements and the properties of each element must be assigned from the bank of standard reference data.

Individual tissue and structures were identfied in MIMICS from individual DICOM images generated by CBCT using a default threshold technique. A radiologist expert also confirmed and corrected the threshold criteria for the identifiable structures. These structures included cancelous and cortical bone, enamel, dentine, and implant. Cementum and dental pulp were excluded because of their relatively low volume and thus minor effects on the analysis.

Figure 4-1 shows one CT image slice of the segment of pig mandible in which the cortical, cancellous, enamel and dentine are shown.

Implant is placed in parallel with the long axis of the 2nd premolar at the centre of the crestal bone. To investigate the relation between soft tissue surrounding the implant and the RF of implant, the soft tissue with different sizes are built in MIMICS and placed in contact areas of implant and bone. Figure 5-1 shows one of CT image slices in which a 3D soft tissue is constructed as 4/8 hallow cylindrical section in interfacing areas of

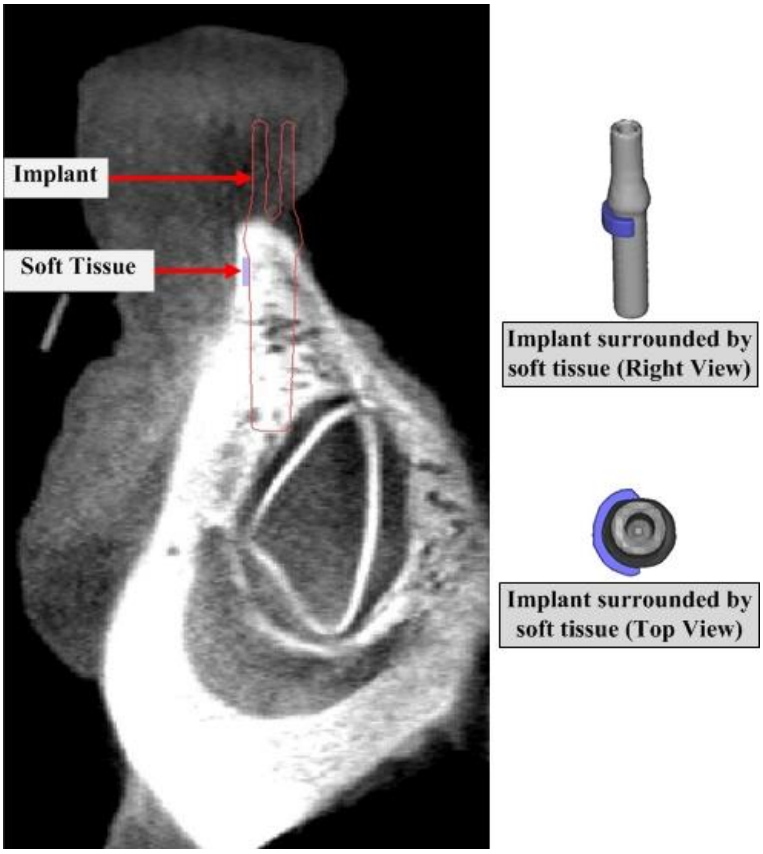

Figure 5-1: A slice of CT image that showing the soft tissue built as 4/8 hollow cylindrical section in interfacing areas of implant and bone

implant and bone.

The 3D section of pig mandible and soft tissue were meshed in MIMICS and imported into ANSYS for RFA. Because of the complixity of the model, 3-D 10-Node tetrahedral structural solid element is used in this analysis. The same element used in chaprter 4 is employed here as well. The same contact surfaces of different parts of 3D model

(cortical, cancellous, enamel, dentine, soft tissue and implant) are all have to move together to prevent the relative motion. Therefore, the coincident nodes are selected to be rigidly fixed.

Material properties of different structures of this model are all assumed homogeneous and isotropic. The material properties of cortical/cancellous bone, soft tissue, enamel, dentine, and dental implant are listed in Table 5-1[40,53].

Table 5-1: Material properties of the partial pig jaw model

	Young's modulus E (Gpa)	Poisson's ratio ϑ	Density ρ $(\frac{kg}{m^3})$
Cortical bone	14	0.3	1300
Cancellous bone	0.49	0.3	1300
Dental implant	104.8	0.342	4430
Enamel	75	0.33	2970
Dentine	15	0.31	2140
Soft tissue	0.01[1]	0.17	1000

[1]In the primary stability, the Young's modolus of the soft tissue changes from 1MPa to 10 MPa [40]. In this study, the Young's modolus of soft tissue is assumed to be 10 MPa.

5.1.2 Parametric studies

5.1.2.1 The effect of the size

To detect the effect of size of soft tissue surrounding the implant on RFof implant, 3D soft tissue (2.5 mm tickness and 2 mm heigth) is built in MIMICS software in the interfacing areas of implant and bone as an approximately 1/8 hollow cylindrical section around the center of implant. The soft tissue increases from 1/8 to 8/8 hollow cylindrical section in 1/8 increment, the tickness and the heigth of soft tissue remain constant for all of these steps and the resonance frequencies of implant are analyzed. For better monitoring of resonance frequency , the 3D soft tissue are also built as 12/13 and 23/24 hollow cylindrical section. Figure 5-2 shows tranverse and coronal views of one of CT images slices when the soft tissue is constructed as 4/8 and 6/8 hollow cylindrical section

around the implant, the 3D models of soft tissue suroudning the implantt are also depicted in Figure 5-2.

In addition, further analysis are carried out to investigate the effect of the size of soft tissue on resonance frequency of implant. Hence, soft tissue is constructed as 2/8, 4/8, 6/8 and 8/8 hollow cylindrical section and the heigth of each case increases from 2 mm to 10 mm in 1 mm increment. The tickness of soft tissue remains constant for all of these steps. Figure 5-3 shows 3D models of two differnt heigths of soft tissue when it is built as 4/8 hollow cylindrical section.

5.1.2.2 The effect of location

In order to investigate the effect of location of soft tissue on resonance frequency of implant, 3D soft tissue (2.5 mm tickness and 2 mm heigth) is built as 2/8 hollow cylindrical section in contacting areas of implant and bone, shown in Figure 5-4, and the the location of soft tissue is changed along negative z axis. In this case the soft tissue is only interfcaed with cortical or cancellous. The resonance frequencies of implant is analyzed in ANSYS simulation environment.

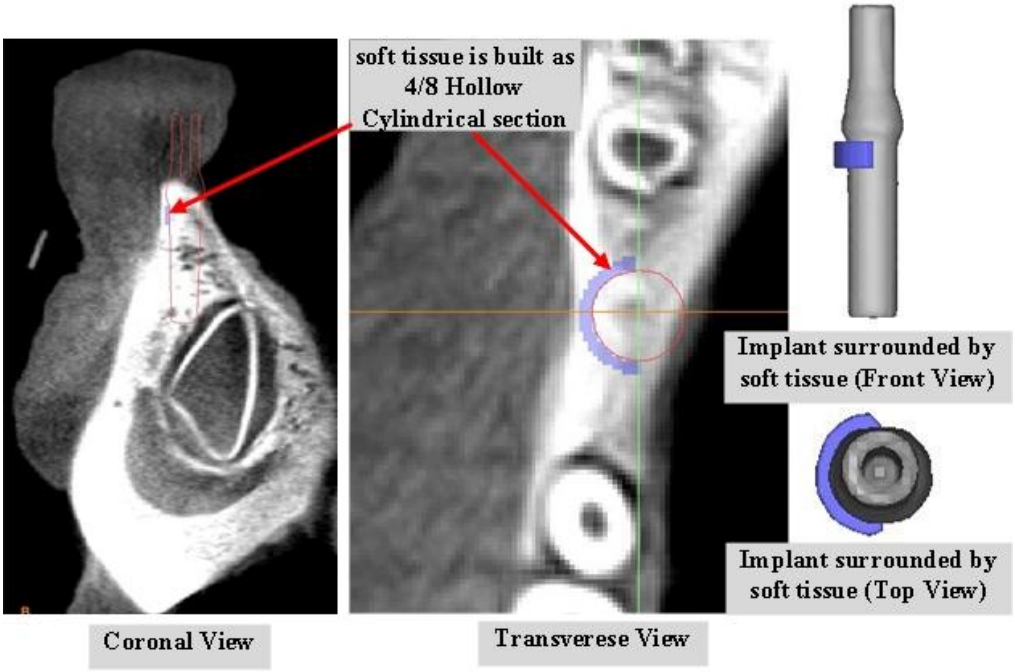

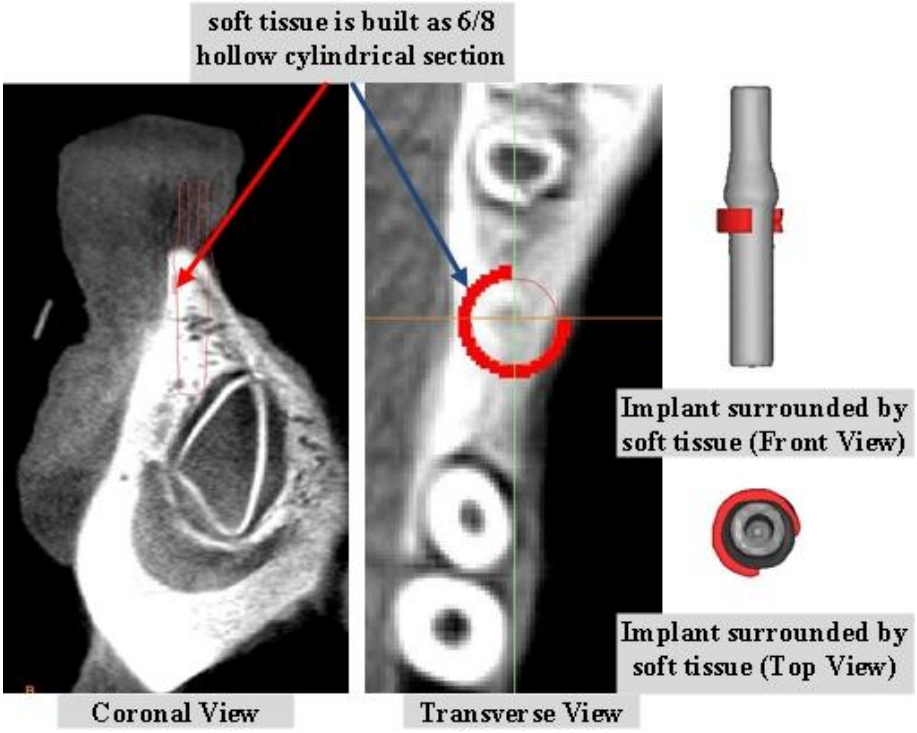

Figure 5-2: Transverse and coronal views of a slice of CT image showing the soft tissue as 4/8 and 6/8 hollow cylindrical section suroudnig the implant, and the 3D models of both implant and soft tissues

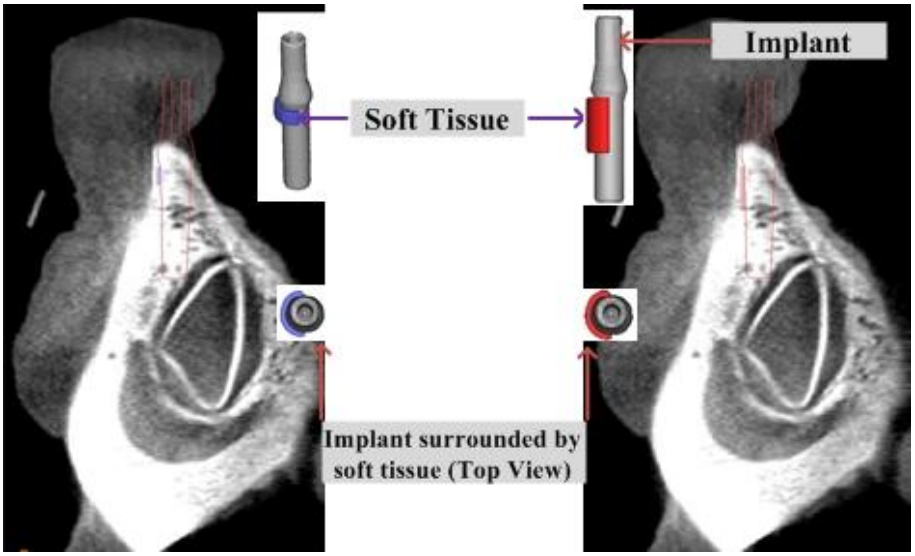

Figure 5-3: 3D modesl of two different heigths of soft tissue when it is built as 4/8 hollow cylindrical section.

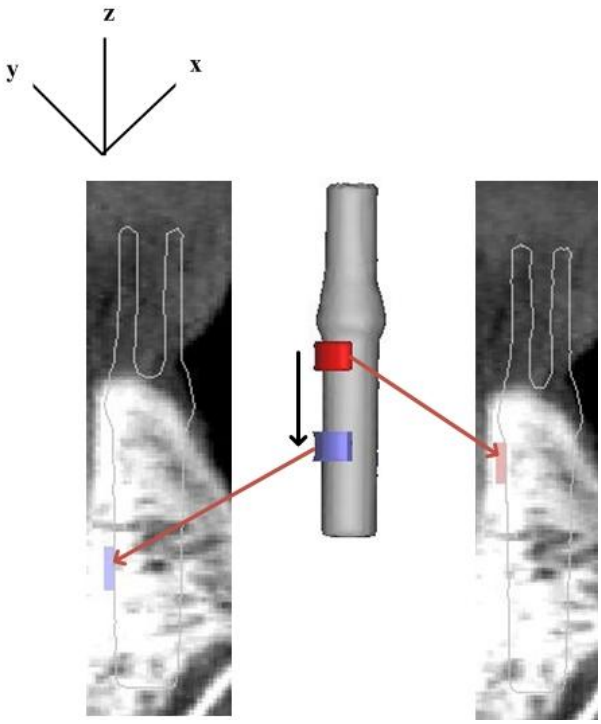

Figure 5-4: 3D soft tissue is constructed as 2/8 hollow cylindrical section and is moved along z axis

Furthermore, the effect of the location of soft tissue on RF of implant is studied in this chapter. To do so, a soft tissue as 1/8 hollow cylindrical section is counstructed and rotated about z axis, as depicted in Figure 5-5. Two mode shapes, No.1 and No.2 are

investigated. In mode shapes No.1 and No.2, the implant rotates around x and y axis repectively. The heigth (4 mm) and the tickness (2.5 mm) of soft tissue remain constant for all directions shown as 1 to 8 in Figure5-5.

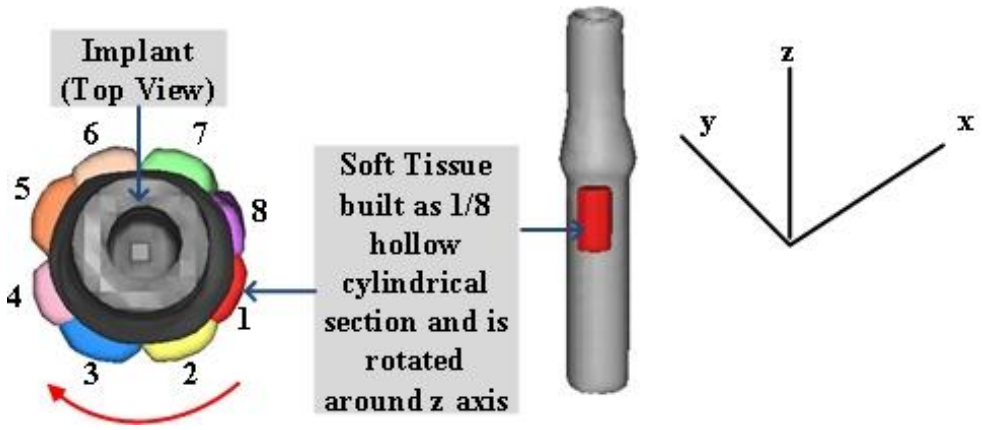

Figure 5-5: 3D soft tissue constructed as 1/8 hollow cylindrical section and rotates around z axis

5.2 Results

The resonance frequencies of implant when the soft tissue (2.5mm tickness and 2 mm heigth) is bulit as an approximtaley 1/8 hollow cylindrical section and increases from 1/8 to 8/8 are listed in Table 5-2 and plotted in Figure 5-6.

Table 5-2: The resonance frequencies corresponding to the soft tissue when it is built as an apporximately 1/8 hollow cylindrical section and increases from 1/8 to 8/8: KHz

	Segment of hollow cylindrical section									
	1/8	2/8	3/8	4/8	5/8	6/8	7/8	12/13	23/24	8/8
Resonnace frequency of implant (KHz)	11.11	11.1	11.078	11.065	11.033	10.936	10.916	10.9	10.895	10.099

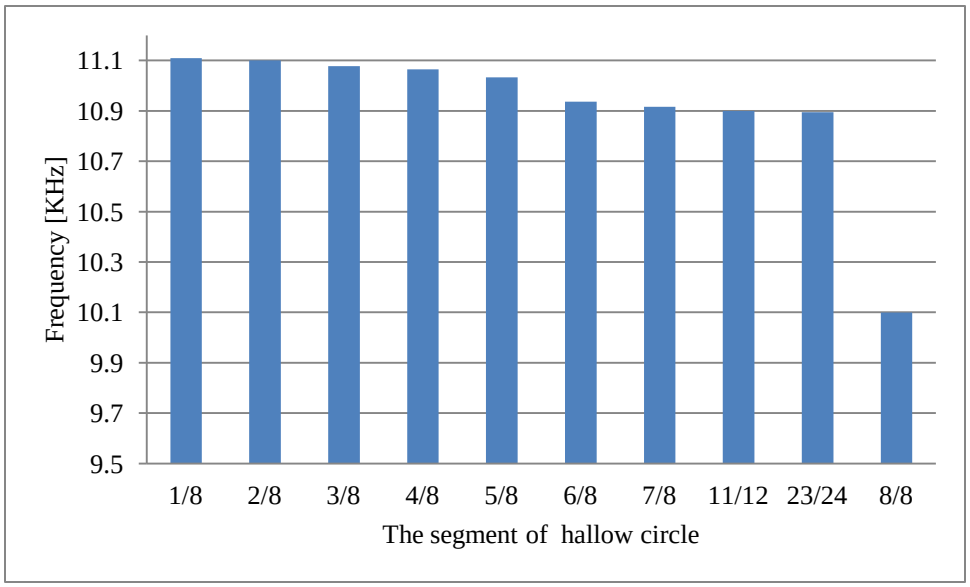

Figure 5-6: The results of the resonance frequencies corresponding to the soft tissue when it is built as an apporximately 1/8 hollow cylindrical section and increases from 1/8 to 8/8

From Figure 5-6, it can be seen that the resonance frequency of implant decreases gradually when the soft tissue surrouding the implant increases. Table 5-2 indicates that the big jump in resonance frequency happens when the 8/8 hollow cylindrical section of soft tissue surrounded the implant. In this stage, the contact areas of implant and bone is surrounded by soft tissue. As the material properties of soft tissue is less than those in cortical and cancellous bone (comparing 0.01 GPa to 0.49GPa and 14GPa), the complete engaging of implant and soft tissue makes a remarkable drop in RF of implant.

The resonance frequencies of dental implant are plotted in Figure 5-7 to Figure 5-11 and listed in Table 5-3 when the soft tissue is constructed as 2/8, 4/8, 6/8 and 8/8 hollow cylindrical section , the heigh of each case increases from 2 mm to 10 mm in 1 mm steps and the tickness of soft tissue keeps constant.

Table 5-3: The resonanace frequencies corresponding to the soft tissue built as 2/8, 4/8, 6/8 and 8/8 hollow cylindrical section and the heigth of each case increases from 2 mm to 10 mm in 1 mm steps: KHz

	Heigth of soft tissue (mm)								
	2	3	4	5	6	7	8	9	10
RF when soft tissue is built as 2/8 circle	11.1	11.09	11.078	11.04	11.022	10.982	10.978	10.977	10.98
RF when soft tissue is built as 4/8 circle	11.065	11.052	10.977	10.949	10.935	10.918	10.916	10.91	10.897
RF when soft tissue is built as 6/8 circle	10.936	10.85	10.65	10.572	10.53	10.51	10.5	10.498	10.496
RF when soft tissue is built as 8/8 circle	10.099	10.02	9.854	9.263	9.214	8.907	8.7	8.7	8.7

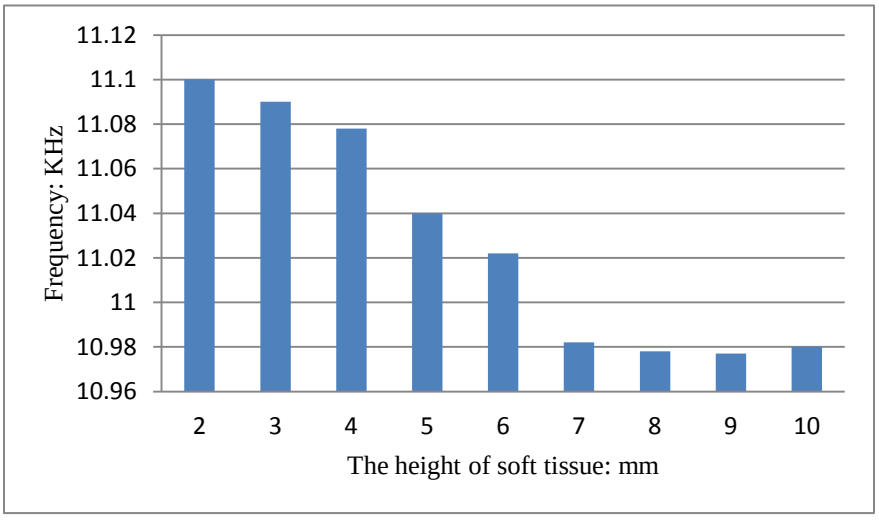

Figure 5-7: The results of the resonance frequencies of implant when the soft tissue is built as 2/8 hollow cylindrical section around the implant and the height of it increases from 2 mm to 10 mm in 1 mm steps

Figure 5-8: The results of the resonance frequencies of implant when the soft tissue is built as 4/8 hollow cylindrical section around the implant and the heigth of it increases from 2 mm to 10 mm in 1 mm steps

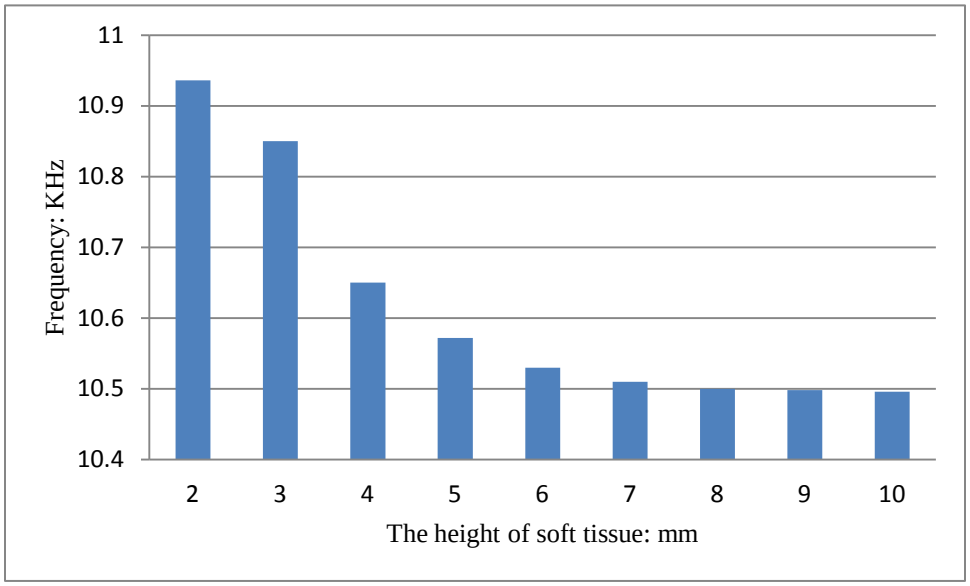

Figure 5-9: The results of the resonance frequencies of implant when the soft tissue is built as 6/8 hollow cylindrical section around the implant and the heigth of it increases from 2 mm to 10 mm in 1 mm steps

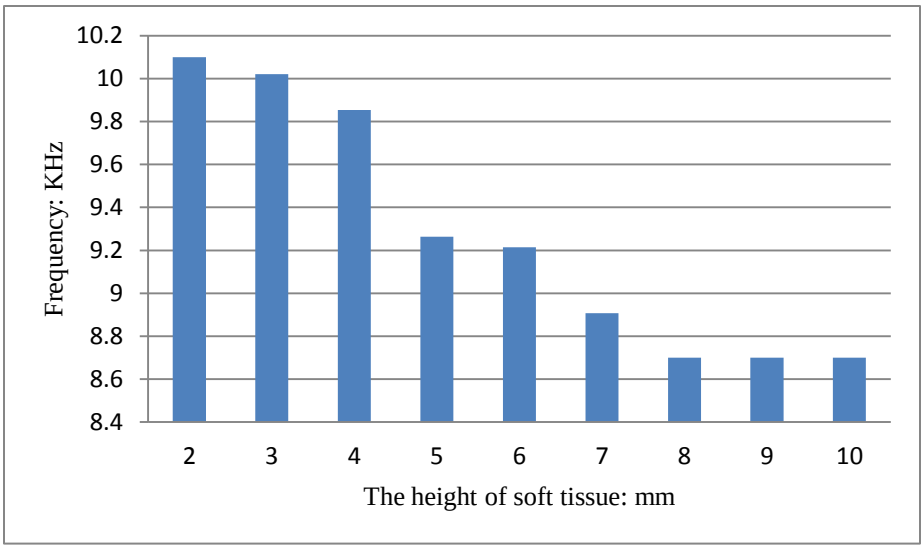

Figure 5-10: The results of the resonance frequencies of implant when the soft tissue is built as 8/8 hollow cylindrical section around the implant and the height of it increases from 2 mm to 10 mm in 1 mm steps

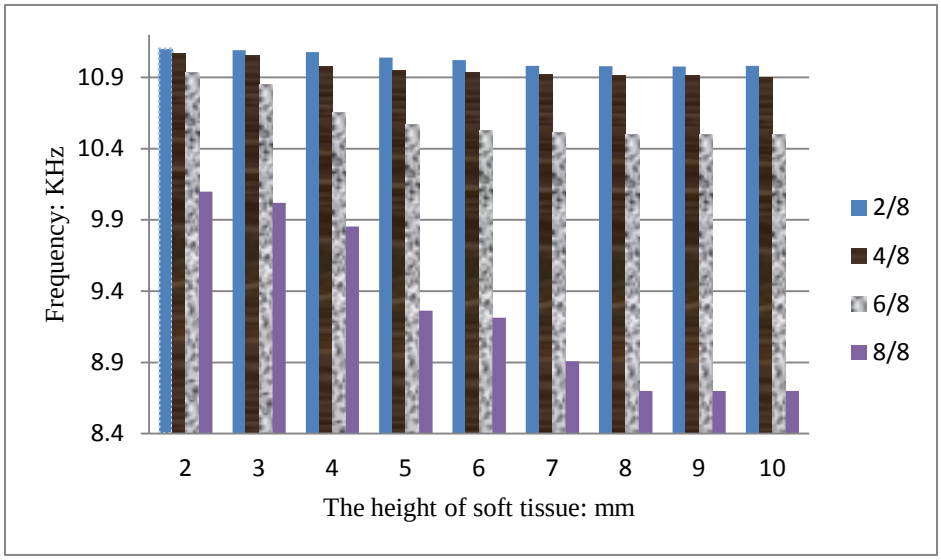

Figure 5-11: The results of the resonance frequencies of implant when the soft tissue is built as 2/8, 4/8, 6/8 and 8/8 hollow cylindrical section around the implant and the height of it increases from 2 mm to 10 mm in 1 mm steps

From the plotted results of Figure 5-7 to Figure 5-11, it is figured out that the resonance frequency of dental implant decreases significantly when the heigth of soft tissue surrounding the implant increases from 2 mm to 7 mm and it reaches a plateaue after 7 mm. In case the heigth of soft tissue is between 2 mm to 7 mm, the soft tissue is

essentially engaged with cortical bone while when it is between 7 mm to 10 mm the soft tissue is interfaced with both cortical and cancellous bone. Therefore, the results indicate that the RF of implant decreases considerbaly when the soft tissue is formed in cortical bone. As it is shown in Figure 5-11 the resonance frequency of implant decreases mainly when the whole contact areas of implant and bone are covered by soft tissue. Even though in all cases the resonance frequency of implant decreases by increasing the heigth of soft tissue surounding the implant in cortical bone, the substantial jump in resonnace frequency happens when the whole contact area of implant and bone is surounded by soft tissue. Comparing the mechanical properties of cortical (Young's modolous of 14Gpa) and cancellous (Young's modolous 0.49 Gpa) to soft tissue (Young's modolous of 0.01 GPa) indicates that the resonance frequency of implant is affected by its boundary condtion material properties. Hence, in addition to the size of soft tissue, the location of soft tissue is also an important factor in changing the RF of implant.

To precisely check the resonance frequencies reduction when the soft tissue is built as 2/8, 4/8, 6/8 and 8/8 hollow cylindrical section, a variable is defined as the absolute difference of the these frequencies by Eq.(5-1), and the values are listed in Table 5-4.

$$d_j^i = \left| f_j^i - f_{j-1}^i \right| \qquad \textbf{(i=1 to 4 , j=2 to 10)} \qquad \textbf{(5-1)}$$

Where d_j^i is the absolute differences of resonance frequecies; f_j^i and f_{j-1}^i are the jth frequency when the soft tissue is built as 2/8 (i=1), 4/8 (i=2), 6/8 (i=3), and 8/8 (i=4) circle.

Table 5-4: The absolute differences of resonance frequencies corresponding to the soft tissue when it is built as 2/8, 4/8, 6/8 and 8/8 circle and the heigth increases from 2 mm to 10 mm : Hz

	2	3	4	5	6	7	8	9	10
RF of 4/8 compares to RF of 2/8	35	38	101	91	87	64	62	67	83
RF of 6/8 compares toRF of 2/8	164	240	428	468	492	472	478	479	484
RF of 8/8 compares to RF of 2/8	1001	1070	1224	1777	1808	2075	2278	2277	2280

From Table 5-4, it can be seen that the significant differences in resonance frequency of implant occurs when the 8/8 hollow cylindrical section case is compared

with 2/8. It can be concluded that in clinical practice, any big change in RF of implant implicates possiblity of growing soft tissue in contacting areas of implant and bone.

The resonance frequencies of implant in case of the soft tissue (thickness 2.5 mm and height 2 mm) is constructed as 2/8 hollow cylindrical section and the location of it moves along negative z axis, Figure 5-4, are listed in Table 5-5 and plotted in Figure 5-12.

Table 5-5: The resonance frequencies corresponding tothe soft tissue when it is built as 2/8 hollow cylindrical section and moves along z axis, Fig. 7: KHz

	$Step^1$								
	45.8-43.8	43.8-41.8	42.8-40.8	41.8-39.8	40.8-38.8	39.8-37.8	38.8-36.8	37.8-35.8	35.8-33.8
Resonance frequency	11.1	11.02	11.015	11.007	10.95	10.959	10.965	10.978	10.975

[1]The numbers showed in steps indicates the transverse position in CT images slices.

Figure 5-12: The resonance frequencies of the soft tissue when it is built as 2/8 hollow cylindrical section and moves along z axis, : KHz

The Figure 5-12 shows that the RF of implant decreases significanly at the border of cortical and cancellous bone. When the soft tissue is formed in cortical bone, the

effectiveness of soft tissue in decreasing the RF of implant is more visiable than when it is formed in cancellous bone.

The resonance frequencies of implant are listed in Table 5-6 and shown in Figure 5-13 when the soft tissue is constructed as 1/8 hollow cylindrical section and rotates around the center of implant, shown in Figure 5-5. In Figure 5-13, the dash line are the mode shapes No.1 and the solid line are the mode shapes No.2. Figure 5-13 shows that the resonance frequencies of implant for the mode shapes that are related to the dash line are higher than those that are related to the solid line. Furthermore, Figure 15 indicates that the direction of soft tissue around the implant will not affect the resonance frequency of implant considerably. For example, when the soft tissue is located in direction 1 and moved to location 2 (Figure 5-5) , the RFs of implant for the mode shape No.1 are 10.912 KHz and 11.102 KHz repectively.

Table 5-6: The perpendicular resonance frequencies corresponding tothe soft tissue when it is built as 1/8 circle and rotates around the center of implant: KHz

	Direction							
	1	2	3	4	5	6	7	8
Implant rotates around y axis	8.798	8.911	8.957	8.853	8.897	8.956	8.772	8.835
Implant rotates around x axis	10.912	11.102	11.082	11.032	10.959	11.125	10.902	10.98

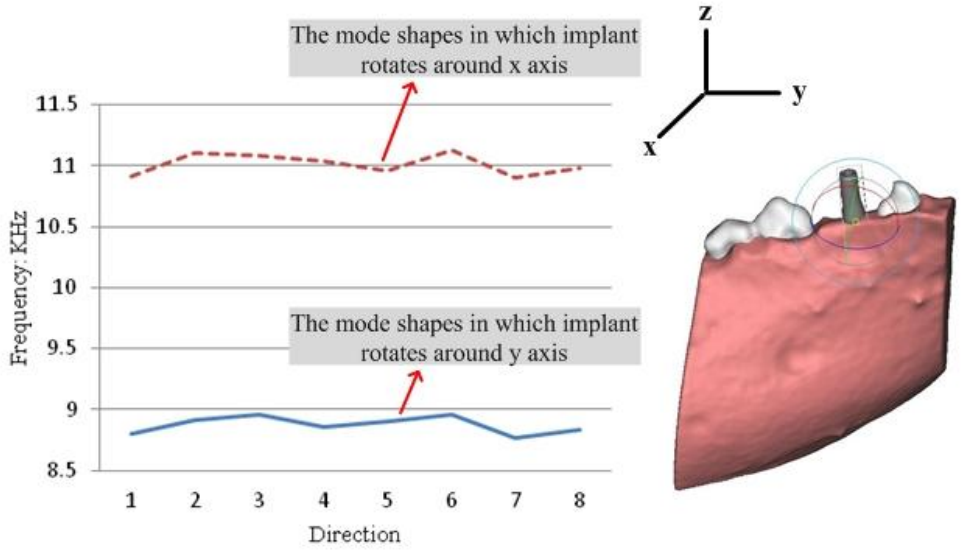

Figure 5-13: The resonance frequencies of the soft tissue when it is built as 1/8 hallow circle and rotates around the center of implant, shown in Figure 5-6: KHz

Figure 5-14 and Table 5-7 show the results of resonance frequencies when the soft tissue (2.5 mm tickness) is formed as 2/8 circle and the heigth of it increases from 2 mm to 10 mm. This is the exactly the same as the case shown in Figure 5-8, but since it is found that the RF of implant decreases when the soft tissue is formed in cortical and reaches a platuea when it grows to cancellous bone, some new cases have been added in the border of cortical to cancellous to better clarify what happens there. When the heigth of soft tissue is 7.8 mm, the soft tissue is fully located in cortical bone and at 8 mm it is engaged with both cortical and cancellous bones.

Table 5-7: The resonance frequencies of implant in case the soft tissue is constructed as 2/8 circle and the heigth of it increases from 2 mm to 10 mm:KHz

	Heigth of soft tissue (mm)											
	2	3	4	5	6	7	7.8	8	8.6	9	9.4	10
RF of implant	11.1	11.09	11.078	11.04	11.022	10.982	10.98	10.978	10.977	10.977	10.978	10.98

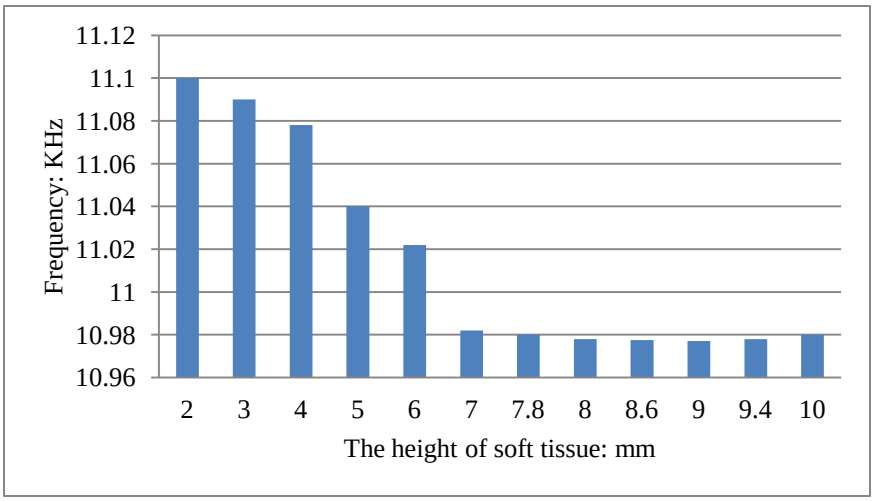

Figure 5-14: The results of resonance frequencies of the soft tissue built as 2/8 circle and the height of it increases from 2 mm to 10 mm

5.3 Discussion

In this study, we used the RFA method to determine the effect of soft tissue surrounding the implant on RF of implant. We found that the resonance frequency of implant is influenced by the size and the location of soft tissue especially when it is formed in cortical bone.

From the calculated results in Figure 5-6 to Figure 5-11 it can be seen that when the soft tissue is formed in cortical bone, the resonance frequency of implant is mainly affected by the size of soft tissue,. When the soft tissue becomes larger in cortical, the resonance frequency decreases significantly but when it passes the border between cortical and cancellous and continues to grow in cancellous bone, the resonance frequency remains constant and reaches a plateau. Theoretically, the resonance frequency of a cantilever beam fixed at one side and free to vibrate at the other end is directly related to the boundary condition variation. This observation can be explained by considering the material properties of cortical, cancellous and soft tissue. It is known that the cortical bone is more rigid than both cancellous and soft tissue (cancellous is harder than soft tissue). Thus, more flexibility in implant-bone integration can be expected when the soft tissue is formed in cortical bone than when it is formed in cancellous bone (Figure 5-12). The lowest resonance frequency in Figure 5-12 happens at the border of

cortical to cancellous bone. The results are in agreement with the results of [56]. They investigated the effect of foundation flexibility on seismic response of reinforced concrete TV-towers and found that the foundation flexibility increases the natural periods, alters the natural mode shapes, and decreases the base bending moment.

5.4 Conclusion

The FEA results indicate that RF of implant decreases because of formation of soft tissue at the implant-bone interface. The RF of implant decreases considerably when soft tissue grows in cortical bone. Moreover, it is found that the RF of implant is not very sensitive to the formation of soft tissue in cancellous bone. Finally, the direction of soft tissue formation in a dental implant does not affect its RF.

6: EXPERIMENTS ON PIG JAW

In numerical approach, we assumed that the material properties of the bone and tissue are all homogenous and isotropic which might not necessarily valid in reality. To observe these effects, *in vivo* studies is carried out in this chapter. The effect of free length of implant on RF has been studied in previous chapters both experimentally (implant placed in a chuck) and numerically (FE method). In this chapter, the effect of some parameters such as free length, and size on RF is investigated. For these experiments, three domestic young adult pig mandibles were obtained from the slaughter house (Britco Pork Inc**.).** A 3.75×11.5 mm MIS endosseous implant is placed in pig mandible No.1. Two different implant sizes, 3.75×13 mm and 4.2×10 mm, are placed in the right and left sides of pig mandible No.2. The last pig mandible is used for placing 3.75×13 mm implant. MIS surgical protocol is followed to place the implants to establish the primary implant stability. In this *in vivo* analysis, implant is buried in the bone and the 'transfer mount' is screwed into implant. The implant is excited by an impulse hammer (Dynapulse model 5800B2, Dytran Instruments Inc., USA). The vibrating signal is recorded by an accelerometer (model 3035BG). A non-contact acoustic microphone (40BE repolarised free field microphone, G.R.A.S sound and vibration, Denmark) is also used to measure impact sound. Both impulse force and the vibrating signal response are transferred to Photon Software for modal analysis. The *in vivo* test set up components including pig mandible, transfer mount, accelerometer, microphone and Photon are shown in Figure 6-1.

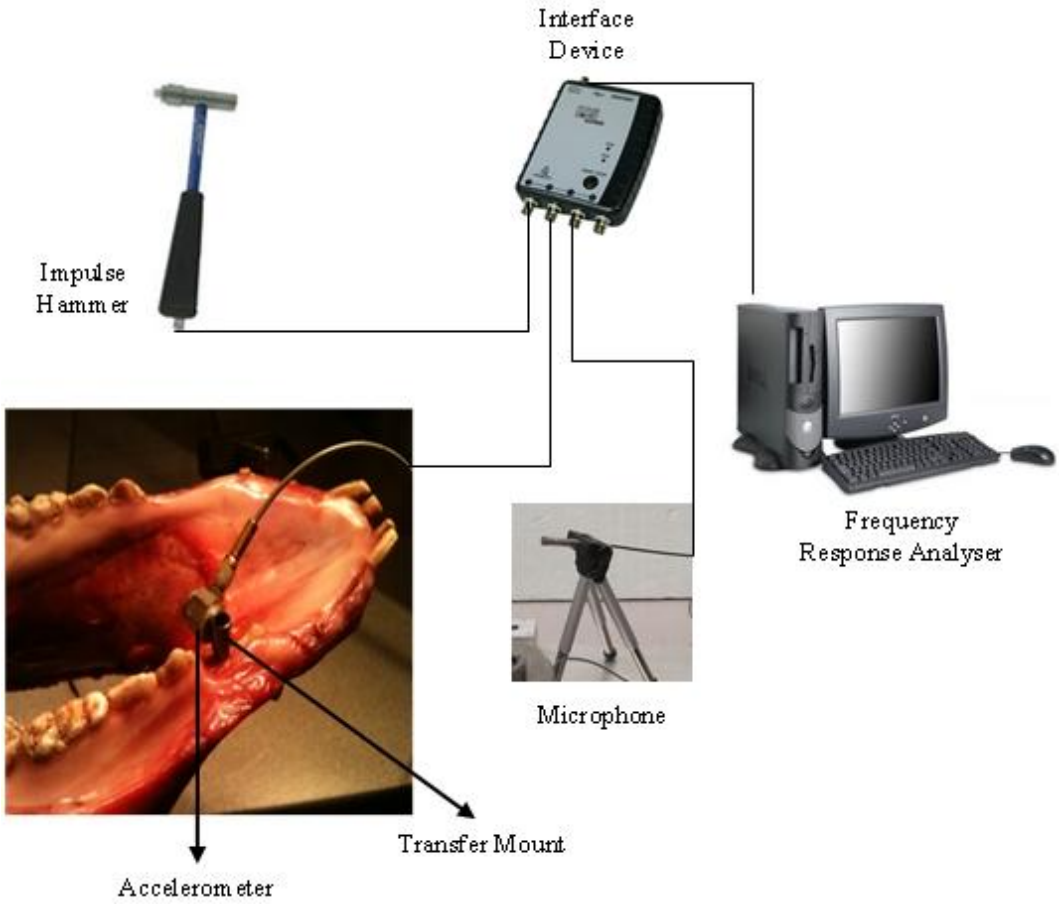

Figure 6-1: *In vivo* test set up

6.1 The effect of implant's free length on RF

The effect of implant's free length on RF is analyzed by using both accelerometer and microphone.

6.1.1 Accelerometer results

The accelerometer is used for recording the vibrating response. The tests are repeated three times, and each test is the average of five impacts. In pig mandibles NO.1 three different implant's free lengths (1.78 mm, 2.29 mm and 2.87mm) are studied. The FFT (Fast Fourier Transform) of vibrating signals are shown in Figure 6-2.

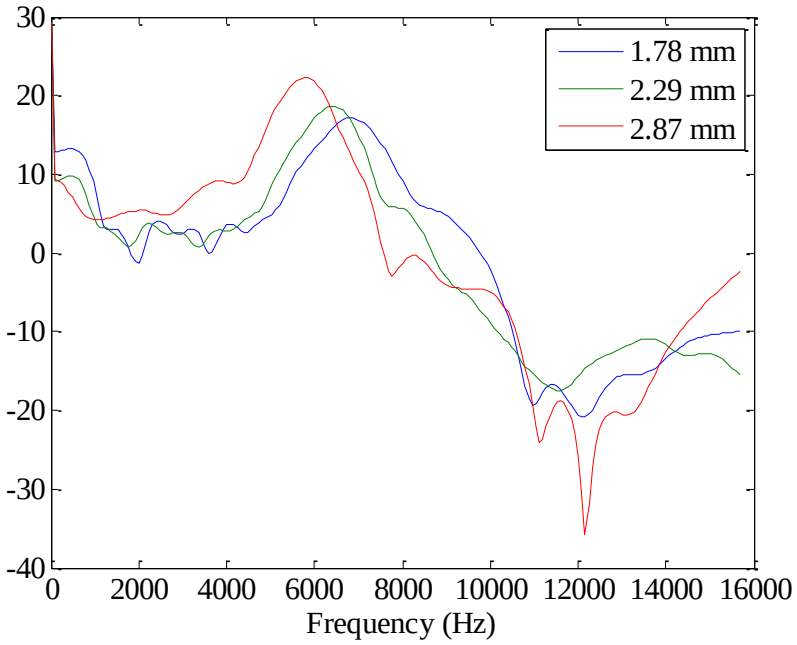

Figure 6-2: The FFT of different free length of implant in pig No.1

The results shows that the RF decreased from (6.8) KHz to (5.84) KHz when the length of implant left out of the bone increased from 1.78 mm to 2.87 mm respectively. It can be concluded that the RF of implant decreases with increasing the free length.

The same conclusion is obtained by studying the effect of free length on the RF of implant in pig mandible NO.2. Two implants (3.75×13 mm and 4.2×10 mm) are placed in the right and left side of the jaw respectively. In these experiments the jaw is fixed by a metal clamp from the opposite side where the implant is placed and the RF is measured for both implants at different free lengths. The results are tabulated in Table 6-1.

Table 6-1: The FFT of different free length of implant in pig No.2

	Free length of implant (mm)		
	2.41	3.07	3.47
RF of implant inserted in right side of jaw (KHz)	7.36	7	6.88
	1.14	2.69	3.12
RF of implant inserted in left side of jaw (KHz)	7.52	7.2	6.8

6.1.2 Microphone results

In pig mandible No.3, 5 different free lengths are tested. The tests are repeated three times, and each test is the average of five impacts. The results are shown in Figure 6-3. The microphone results showed that the RF of implant increases by decreasing the free length.

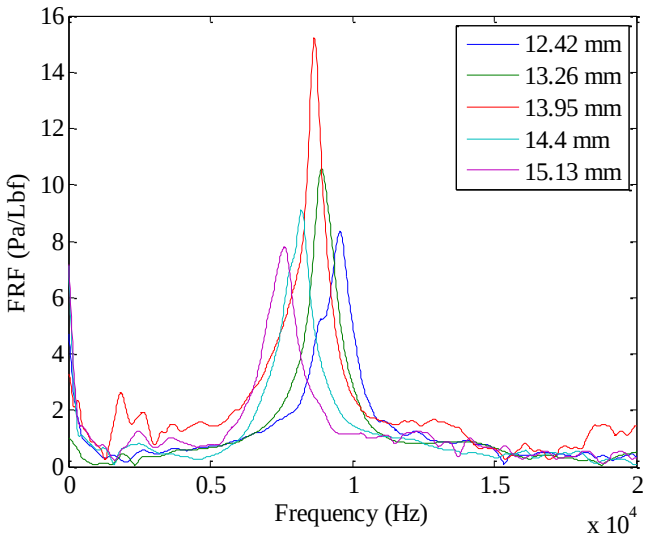

Figure 6-3: The FFT of different free length of implant in pig No.3

6.2 The effect of implant size on RF

The size of implant is determined by its diameter and length. Implant diameter is the dimension measured from the peak of the widest thread to the same point on the

opposite side of the implant. Currently available implants vary in diameter from 3 to 7 mm. The requirements for implant diameter are based on both surgical and prosthetic requirements. Implant length is the dimension from the platform to the top of implant. It has been an axiom in implant dentistry that longer implants guarantee better success rates and prognosis. Although a linear relationship between length and success rate has not been proven, studies have shown that shorter implants have statistically lower success rates [57].

The effect of implant size on RF is analyzed in this section. Both implants buried in the left and right sides of pig mandible No.2, are excited by impulse hammer and the vibration signals are collected by the accelerometer and analyzed by Photon. The results showed that the size of implant is one of the factors that influence the RF. The In summary, the longer implant showed higher RF. In this analysis the RF of implant placed in the right side of pig jaw (3.75×13 mm), is approximately 8 KHz and the RF for the left side implant (4.2×10 mm) is 7.7 KHz.

6.3 Comparison between the RF of implant inserted in a segment and whole pig mandible

The pig mandible No.2 is cut and a segment of it is included the implant (see Figure 6-4) is tested. The same method used for other tests is used to acquire the RF. The RF for the whole and partial pig mandibles are shown in Figure 6-4. As it is shown in the Figure 6-4, the RF of implant is the same in both cases. This finding is useful for justifying model reduction in FEM analysis. Comparing with the whole mandible, the segment pig mandible has less number of nodes and elements and thus the analyzing process will be faster.

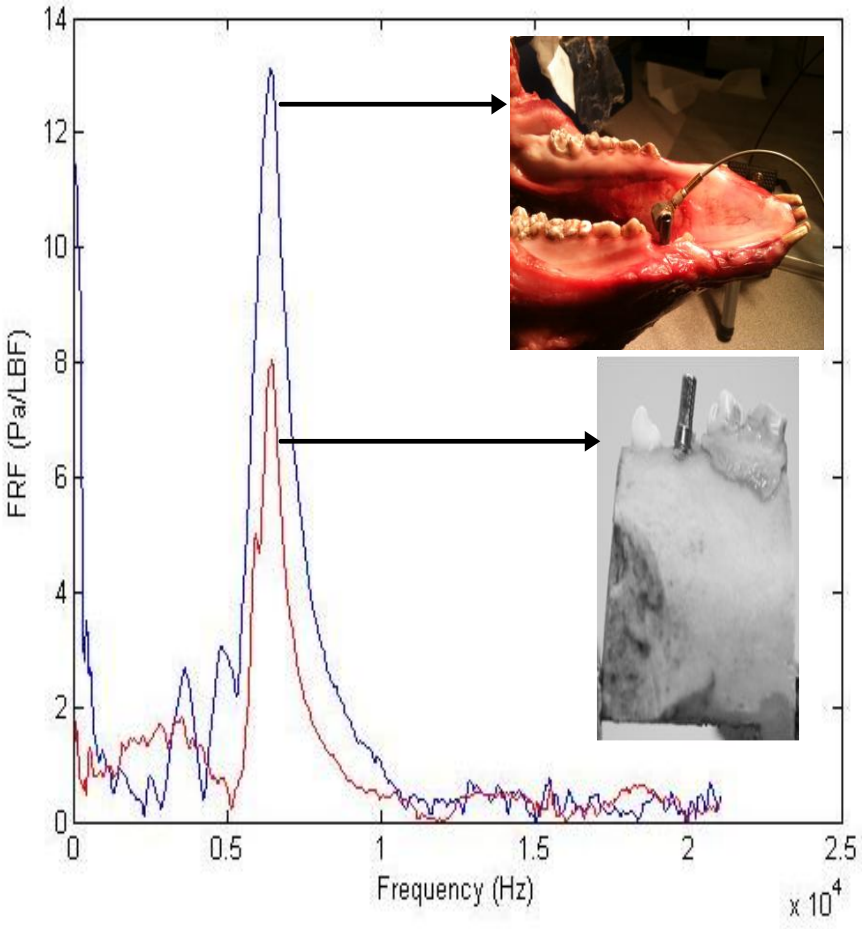

Figure 6-4: Comparison between the RF of implant in selected and whole pig mandible

7: EXPERIMENTAL STUDIES TO FIND THE EFFECT OF SURROUNDING SOFT TISSUE ON RF OF IMPLANT

Soft tissue is a body part that connects, supports, or surrounds other structures and organs of the body, excluding bone. The influence of soft tissues, joints and the fibula on the human tibia's natural frequency have been reported by Van der Perre *et al*. [58,59] and Cornelissen *et al*. [60,61]. They concluded that the major factors that influence the results was the mass and damping effect of muscles. Tsuchikane *et al*. [62] investigated the influence of joints and soft tissue on the RF of the human tibia using the impulse response method combined with modal analysis. Their findings indicate that soft tissue, joint and fibula play a role in damping vibration. They suggested that a change in the RF of the tibia represents a change in the condition of the tibia itself. In dental applications, it is expected that soft tissue affects the RF of implant and little is known about this effect.

In this chapter, an experimental study is conducted to investigate the influences of the surrounding soft tissue on the RF of the implant. It is found that the RF of implant decreases when it is surrounded by soft tissue. Moreover, the results show that the angle between the direction of excitation and the location of soft tissue affects the RF.

7.1 Material and Methods

As shown in Figure 7-1a, a 3.75×11.5 mm MIS endosseous implant is fixed by a rotating metal chuck stand, capable of rotating 360 degree about its' center. A piece of rubber is attached to the dental implant to represent the effect of soft tissue (similar to soft tissue, rubber is both elastic and viscous). As depicted in Figure 7-1, rubber adheres perfectly to the implant. The implant is excited by an impulse force applied by an inverted pendulum. To improve the quality of impact forces, a conical impact tip is fabricated and installed. The impact force applied to the implant is measured by a force sensor (Dytran model 1022V) inserted at the end of the device. The intensity of transient

force remains constant for all tests since the pendulum is released at the same height for all experiments. When the impact head hits the implant, the force sensors triggers the impact and the microphone begins collecting acoustic signal. Here, all the tests are repeated three times when the chuck is rotated about its center from 0^0 to 360^0 (Figure 7-1c) in 10^0 increments. Each incremental rotation of the chuck changes the angle between the direction of impact force and the location of the rubber. The FRF of the microphone signals are calculated by a program written in MATLAB. The sharp peak of the FRF shows the resonance frequency of the implant. The test is also repeated when the rubber is removed and the implant is in fully contacted with the metal chuck.

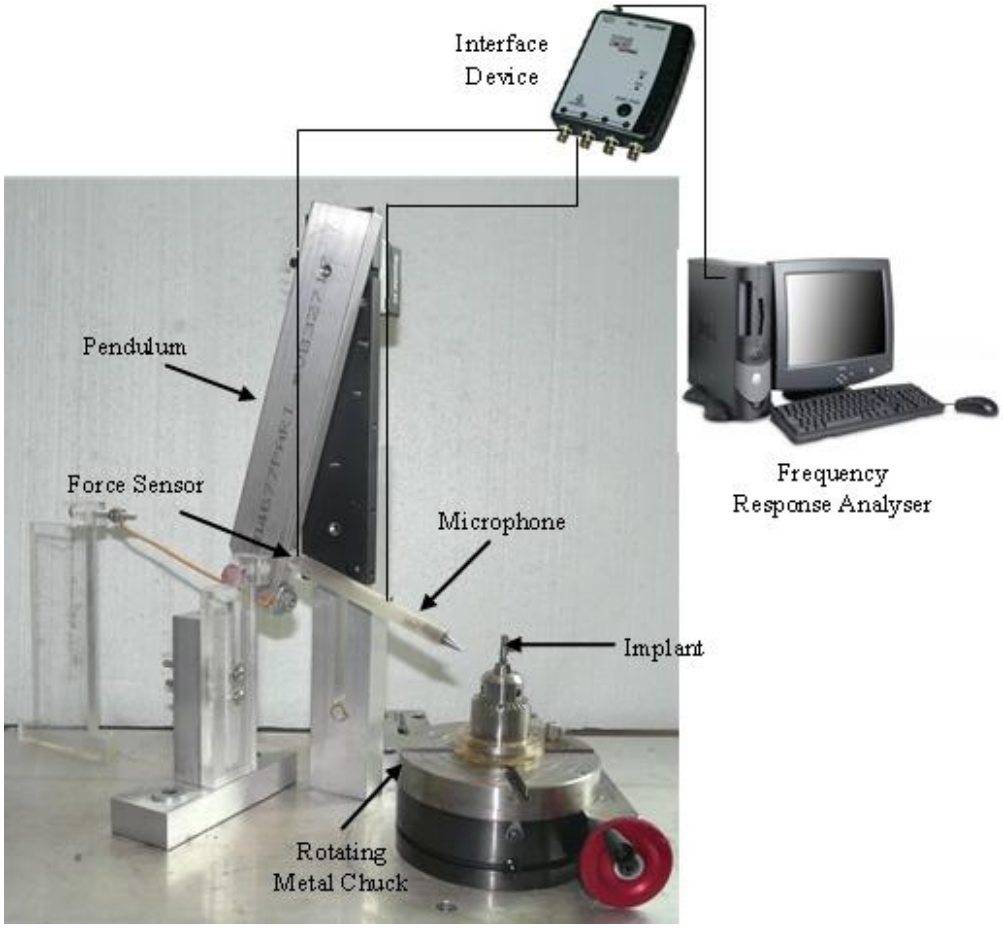
Interface
Device
Pendulum
Force Sensor
Microphone
Implant
Rotating
Metal Chuck
Frequency
Response Analyser

(a)

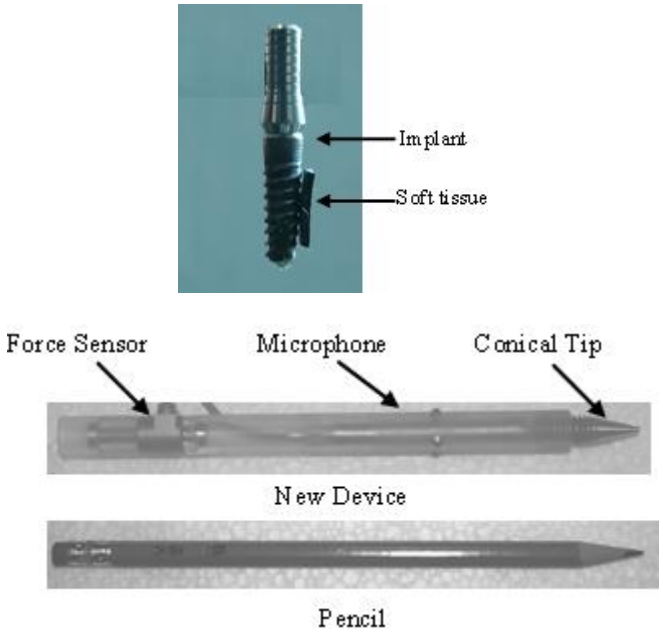
Implant
Soft tissue
Force Sensor
Microphone
Conical Tip
New Device
Pencil

(b)

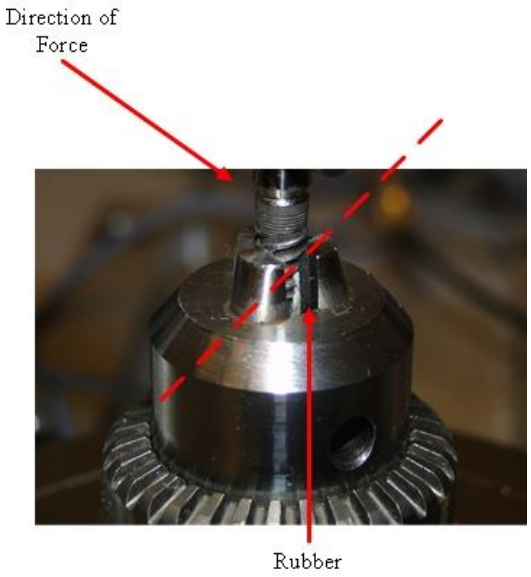

(c)

Figure 7-1: Test set up

7.2 Results

Figure 7-2a and b show a sample FRF of the microphone with and without rubber for the angle 100^0.

The RFs of implant when the chuck is rotated from 0^0 to 360^0 around its centre in 10^0 increments are depicted in Figure 7-3. The minimum, maximum, mean value and standard deviation are shown in this figure. The tests with the rubber is indicated by a dash line, and the tests without the rubber are shown by a solid line.

The results show that the RF of implant decreases when the rubber is attached. For the case with the rubber, the RF at 100^0 has a mean value of 7.88 KHz, and 9 KHz when fully interfaced with the metal chuck. As it is shown in Figure 7.4, the mean value of RF of implant when it has the rubber is approximately 8.1 KHz while it is 8.77 KHz without it. From Figure 7-3 it can be seen that the difference between the RF of implant, with and without rubber at certain degrees are bigger. At these angles, the angle between the direction of impact and the location of the soft tissue are much closer than other angles. When the rubber and impact are in the same direction, the implant has lower RF compared to other angles.

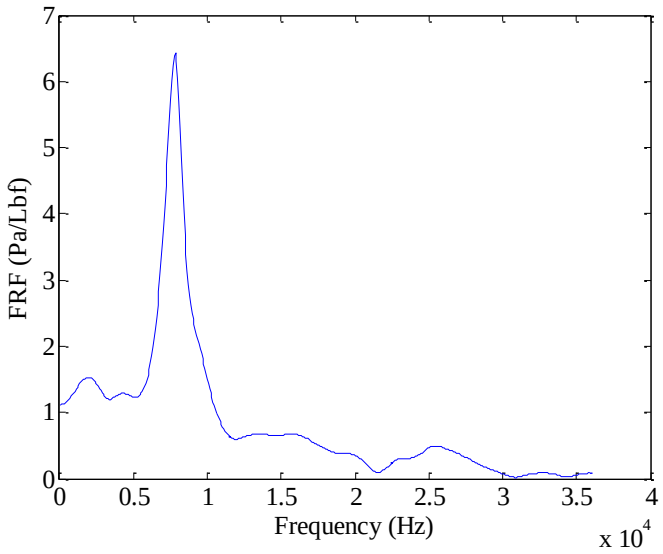

(a)

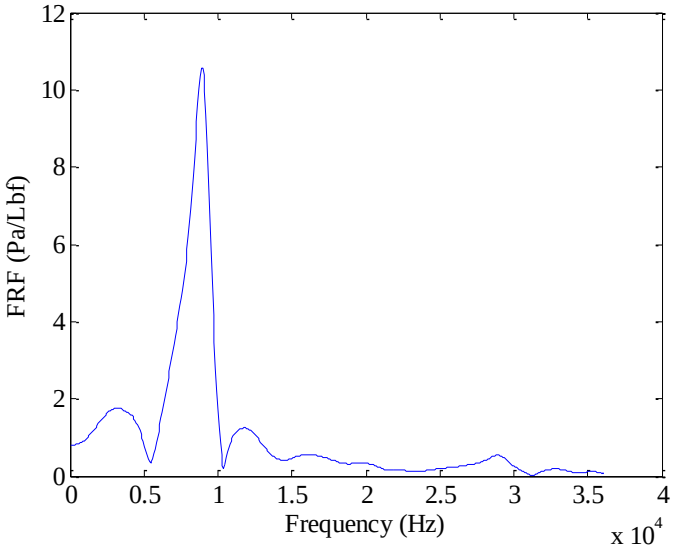

(b)

Figure 7-2: (a) FRF of microphone when the soft tissue is removed and the implant is contacted with metal chuck (b) FRF of microphone when the soft tissue is adhered to the implant and the chuck is rotated 100^0 around its centre

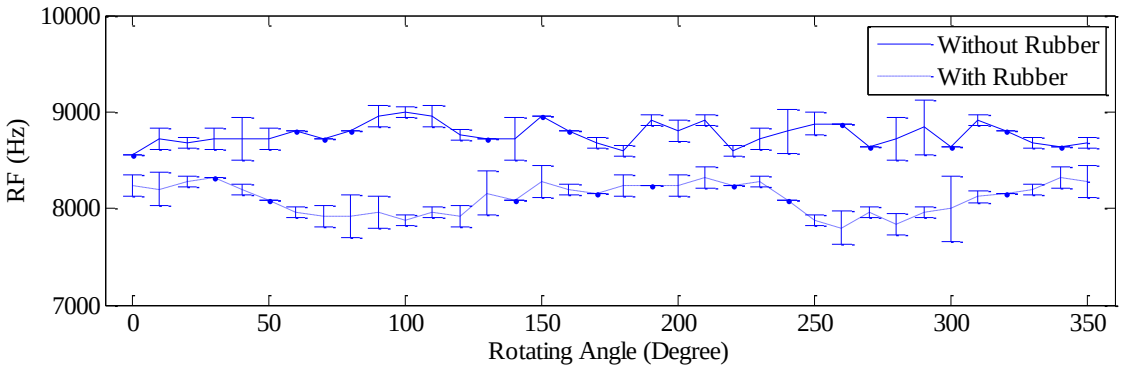

Figure 7-3: The RFs of implant when the chuck is rotated from 0^0 to 360^0 around its centre in 10^0 increments

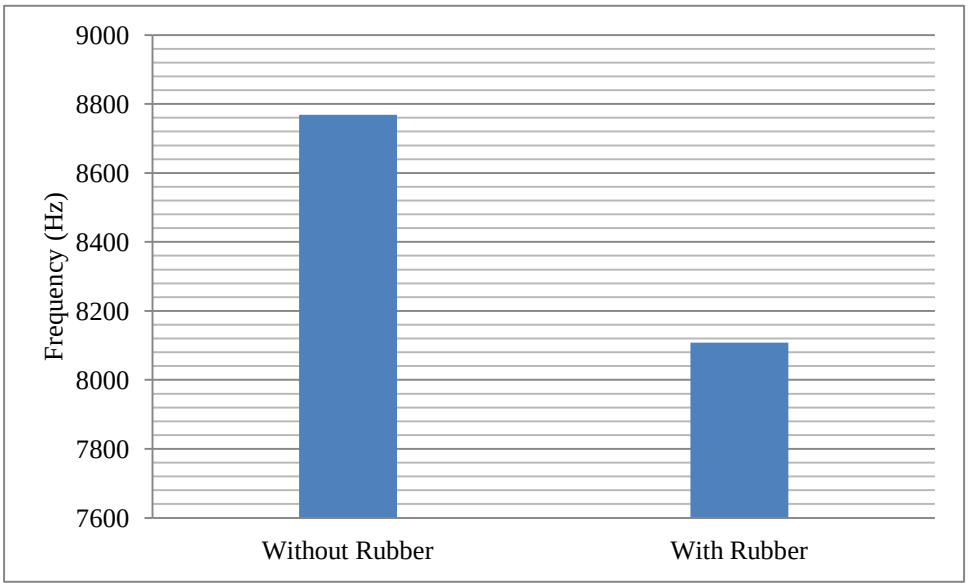

Figure 7-4: The mean values of RFs of implant when the chuck is rotated from 0^0 to 360^0 around its centre in 10^0 increments

7.3 Conclusion

The influences of the surrounding soft tissue on the RF of implant are investigated using the impulse response method.

It is shown that the soft tissue influences the RF. This finding suggests that a change in the RF of an implant represents a change in the boundary condition. The results also demonstrate that the RF is mainly affected by the angle between the direction of the

impact and the location of the soft tissue. When the soft tissue and the impact force are in the same direction, the RF is the lowest. This finding could be used in dental application to predict approximately the location of defect in bone implant integration.

8: CONCLUSIONS AND RECOMMENDATIONS

In order to develop techniques and strategies for assessing dental implant stability numerical modelling is a strong method that has been widely used in recent years. In this thesis, both experimental and numerical results show that the resonance frequency of a coupled implant/chuck is influenced by the material property of each individual units as well as the quality of their integration. Moreover, it is found that the RF of the implant increases when the implant and bone are more integrated, and RF reaches to a plateau when the implant-bone interface is fully integrated.

We also found that the resonance frequency of implant is strongly influenced by the cortical to cancellous bone ratio (CCBR) in the interfacing areas of implant and bone.

The computational results also confirm that RF method is useful in determining the effect of soft tissue on implant stability. It is shown that the resonance frequency of implant decreases considerably when soft tissue volume grows in the cortical bone. Moreover, it is found that the resonance frequency of implant is not sufficient sensitive when the soft tissue is formed in cancellous bone. Experimental results show the remarkably influence of soft tissue on RF of an implant. This finding suggests that a change in the RF of an implant represents a change in the boundary condition of the bone. The results also demonstrate that the RF is mainly affected by the angle between the direction of the transient force and the location of the soft tissue.

In addition, the size of implant is shown to have an important role in determining the RF of implant. It is found that, the resonance frequency of implant is increases when the free length of implant is decreased.

The usability of this method is applicable not only to dental implant but to also other categories of implant such as hip implant to check the stability of implant and realize the integration process. In general, the results of this study can be insightful for

future research. For the future works, it is possible to integrate the 3D pig jaw model in order to investigate the effect of some parameters such as material properties of bone on RF of implant.

.

9: REFERENCE LIST

1. Capek L, Simunek A, Slezak R, Dzan L (2009) Influence of the orientation of the Osstell® transducer during measurement of dental implant stability using resonance frequency analysis: A numerical approach. Med Eng Phys 31:764–9
2. Poul Holm-Pedersen, Niklaus P.Lang, Frauke Muller (2007) What are the longevities of teeth and oral implants? Clin. Oral Impl. Res. 18:15-19
3. Koller B, Att W, Strub JR (2011) Survival rates of teeth implants and double crown-retained removable dental prostheses systematic literature review. Int J Prosthodont 24:109-17
4. Chung WE, Rubestien JE, Phillips KM, Raigrodski AJ (2009) Outcomes assessment of patients treated with osseointegrated dental implants at the university Washington Graduate Prosthodontic Program,1988 to 2000. Int J Oral maxillofac Implants 24:927-35
5. Brunski JB. (1992) Biomechanical factors affecting the bone-dental implant interface. Clin Mater 10:153-201
6. Sennerby L, Roos J. (1998) Surgical determinants of clinical success of osseointegrated oral implants: A review of the literature. Int J Prosthodont 11:408-20
7. Jensen O. (1994) The carter hypothesis. In: Burser D, dahlin C, Schenk RK(eds). Guided bone regeneration in implant dentistry. Hong Kong:Quintessence, 238:239
8. Mihoko Atsumi, Sang-Hoon Park, Hom-Lay Wang (2007) Methods used to assess implant stability status. The International Journal of Oral & Maxillofacial Implants 22:743-754
9. Meredith, N., Shagaldi, F., Alleyne, D., Sennerby, L., Cawley, P. (1997) The application of resonance frequency measurements to study the stability of titanium implants during healing in the rabbit tibia. Clinical Oral Implants Research 8:234–243
10. Hermann JS. , Schoolfiled JD, Nummikoski PV., Buser D, Schenk RK, Cichran DL (2001) Crestal bone changes around titanium implants: a methodology study comparing linear radiographic with histometric measurements. Int J Oral Maxillofac Implants 16:475-85
11. Goodson JM,Haffajee AD, Socransky SS. (1984) The relationship between attachment level loss and alveolar bone loss. J Clin Periodontol 11:384-359
12. Johansson P, Strid K (1994) Assessment of bone quality from cutting resistance during implant surgery. Int J Oral Maxillofac Implants 9:279-288

13. Friberg B, Sennerby L, Roos J, Johansson O, Strid CG, Lekholm U (1995) Evaluation of bone density using cutting resistance measuremnts and microradiography: An in vitro study in pig ribs. Clin Oral Implants Res 6:164-171

14. Roberts WE, Smith RK, Zilberman Y, Mozsary PG, Smith RS (1984) Osseous adaption to continuous loading of rigid endosseous implants. Am J Orthod. 86:95-111

15. Sullivan DY, Sherwood RL, Collins TA, Krogh PH. (1996) The reverse torque test: A clinical report. Int J Oral Maxillofac Implants 11:179-185

16. Lim S, Cha J, Hwang C. (2008) Insertion Torque of Orthodontic Miniscrews According to Changes in Shape, Diameter and Length. Angle Orthod 78:234-240

17. Turkyilmaz I, Tumer C, Ozbek E, Tozum T. (2007) Relations between the bone density values from computerized tomography, and implant stability parameters: a clinical study of 230 regular platform implants. J Clin Periodontol 34:716-722

18. Kaneko T. (1991) Pulsed oscillation technique for assessing the mechanical state of the dental implant-bone interface. Bio-materials 12:555-560

19. Kaneko T,Nagai Y, Ogino M, Futami T, Ichimura T (1986) acoustoelastic technique for assessing the mechanical state of the dental implant-bone interface. J Biomed Mater Res 20:169-176

20. Aoki H (1987) The mobility of healthy teeth as measured with the impact hammer method. Kanagawa Shigaku 22:13-31

21. Hirakawa W (1986) An attempt to measure tooth mobility in terms of time domain wave forms. Kanagawa Shigaku 21:529-543

22. Matsuo E, Hirakawa K, Hamada S. (1989) Tooth Mobilitt measuremet technique using ECM impact hammer method. Bull Kanagawa Dent Coll 17:9-19

23. Manz M, Morris H, Ochi S. (1992) An evaluation of the Periotest system. Part I: Examiner reliability and repeatability of readings. Imp Dent 1:142-146

24. Salvi G, Lang N. (2004) Diagnostic parameters for monitoring peri-implant conditions. Int J Oral Maxillofac Implants 19:116-127

25. N. Meredith, D. Alleyne, P. Cawley (1996) Quantitative determination of the stability of the implant-tissue interface using resonance frequency analysis. Clin Oral Impl Res 7: 261-267

26. Huwiler MA, Pjetursson BE, Bosshardt DD, Salvi GE, Lang NP (2007) Resonance frequency analysis in relation to jawbone characteristics and during early healing of implant installation. Clin Oral Impl Res 18:275–80

27. Tozum TF, Turkyilmaz I, Yamalik N, Karabulut E, Eratalay K (2007) Analysis of the potential association of implant stability, laboratory, and image-based measures used to assess osteotomy sites: early versus delayed loading. J Periodontol 78:1675–82

28. Meredith, N., Book, K., Friberg, B., Jemt, T., Sennerby, L. (1997) Resonance frequency measurement of implant stability in vivo. A cross-sectional and

longitudinal study of resonance frequency measurements on implants in the edentulous and partially dentate maxilla. Clinical Oral Implants Research 8:226–233

29. Bischof, M., Nedir, R., Szmukler-Moncler, S., Bernard, J.P., Samson, J. (2004) Implant stability measurement of delayed and immediately loaded implants during healing. Clinical Oral Implants Research 5:529–539.

30. Glauser, R., Sennerby, L., Meredith, N., Ree, A., Lundgren, A., Gottlow, J., Ha¨ mmerle, C.H.F. (2004) Resonance frequency analysis of implants subjected to immediate or early functional occlusal loading. Clinical Oral Implants Research 15:428–434

31. Rasmusson,L., Meredith,N., Cho, H.I. & Sennerby (1999) The influence of simultaneous versus delayed placement on the stability of titanium implants in onlay bone grafts: a histologic and biomechanics study in the rabbit. International Journal of Oral and maxillofacial Surgery 28:224-231

32. Huang, H.M., Chiu, C.L., Yeh, C.Y., Lin, C.T., Lin, L.H., Lee, S.Y. (2003) Early detection of implant healing process using resonance frequency analysis. Clinical Oral Implants Research 14:437–443

33. Huang, H.M., Cheng, K.Y., Chen, C.H., Lin, C.T., Lee, S.Y. (2005) Design of a stability-detecting device for dental implants. Proceedings of the Institution of Mechanical Engineering—Part H—Journal of Engineering in Medicine 219:203–211

34. Huang, H.M., Pan, L.C., Lee, S.Y., Chiu, C.L., Fan, K.H., Ho, K.N. (2000) Assessing the implant/bone interface by using natural frequency analysis. Oral Surgery, Oral Medicine, Oral Pathology, Oral Radiology, and Endodontics 90: 285–291

35. Lee SY, haung HM, Lin CY,Shih YH (2000) In vivo and in vitro natural frequency analysis of peridontal conditions: An innovative method. J Periodontol 71:632-640

36. Huang HM, Chiu CL,Yeh CY, Lee SY (2003) Factors influencing the resonnace frequency of dental implants. J Oral Maxillofac Surg 61:1184-1188

37. Huang HM, Lee SY, Yeh CY, LIn CT (2002) Resonnace frequency assessemnt of dental implant stability with various bone qualities: A numerical approach. Clin Oral Implants Res 13:65-74

38. Zix J, Hug S, Kessler-Liechti G, Mericske-Stern R (2008) Measurement of dental implant stability by resonance frequency analysis and damping capacity assessment: comparison of both techniques in a clinical trial. Int J Oral Maxillofac Implants 23:525-530

39. Williams, K.R. & Williams, A.D.C. (1997) Impulse response of a dental implant in bone by numerical analysis. Biomaterials 18: 715–719

40. S. Wang, G.R. Liu, K.C. Hoang, Y. Guo (2011) Identifiable range of osseointegration of dental implants through resonance frequency analysis. Med Eng Phys 32:1094–1106.

41. De Almeida, M. S., Maciel, C. D., and Pereira, J. C. (2007) Proposal for an ultrasonic tool to monitor the osseointegration of dental implants. Sensors 7:1224–1237

42. Mathieu, V., Anagnostou, F., Soffer, E., and Haiat, G. (2011a) Ultrasonic evaluation of dental implant biomechanical stability an in vitro study. J. Acoust. 37:262–270

43. Daniel Inman (2008) Engineering Vibration. 3rd edition Pearson, Prentice Hall.

44. Ewins (2000) Modal testing : theory, practice and application. 2nd edition Research Studies Press .

45. Meredith N. (1998) Assessment of implant stability as a prognostic determinant. Int J Prosthodont 11:491-501

46. Meredith, N., Shagaldi, F., Alleyne, D., Sennerby, L., Cawley, P. (1997) The application of resonance frequency measurements to study the stability of titanium implants during healing in the rabbit tibia. Clinical Oral Implants Research 8:234–243

47. Thomson, W.T., (1988) Free vibration. In: Thomson, W.T., ed. Theory of Vibration with Applications, 3rd edition. New York: Prentice-Hall Inc.

48. Lindh T, Gunne J, Tiliberg A, Molin M. (1998) A meta-analysis of implants in partial edentulism. Clin Oral Implants Res 9; 80- 90

49. Holm-Pedersen P, Lang Np, Muler F. (2007) What are the longevities of teeth and oral implants? Clin Oral Implants Res 18:1 5-19

50. Pjetursson BE, Tan K, Lang NP, Bragger U, Egger M, Zwahlen M. (2004) A systematic review of the survival, and complication rates of fixed partial dentures (FPDs) after an observation period of at least 5 years- Implant-supported FPDs., Clin Oral implants Res 15:625-642

51. Eduardo Piza Pellizzer Pellizzer EP, Falcón-Antenucci RM, de Carvalho PS, Sánchez DM, Rinaldi GA, de Aguirre CC, Goiato MC (2011) Influence of Implant Angulation With Different Crowns on Stress Distribution. The Journal of Craniofacial Surgery 22:434-437

52. Roberto Sorrentino, Enrico Felice Gherlone, Gaetano Calesini, Fernando Zarone (2010) Effect of Implant Angulation, Connection Length, and Impression Material on the Dimensional Accuracy of Implant Impressions: An In Vitro Comparative Study. Clinical Implant Dentistry and Related Research 12:63-76

53. Integrated Biomaterial Science, edited by R. Barbucci. Kluwer academic/Plenum publishers, New York, 2002

54. Ernsanli S, Karabuda C, Becj F, Leblebicioglu B. (2005) Resonance frequency analysis of one-stage dental implant stability during the Osseointegration period. J Peridontol 76:1066-1071

55. Lacroix D, Prendergast PJ, Li G, Marsh D. (2002) Biomechanical model to simulate tissue differentiation and bone regeneration: application to fracture healing. Med Biol Eng Comput 40:14-21

56. A. Halabian, M.H. El Naggar (2001) Effect of foundation flexibility on seismic response of reinforced concrete TV-towers. Can. J. Civ. Eng. 28:465-481
57. Winkler S, Morris HF, Ochi S. (2005) Implant survival to 36 months as related to length and diameter. Ann Periodontol 5:22-31
58. Van der Perre, G., Van Audekercke, R, Martens, M. and Mulier, J. C. (1983) Identification of the *in uivo* vibration modes of human tibiae by modal analysis. J. Biomech. Engng, 105:244-248
59. Van der Perre, G. and Cornelissen, P. (1983) On the mechanical resonance of human tibia in vivo. J. Biomechanics 16:549-552
60. Cornelissen, M., Cornelissen, P. and Van der Perre, G. (1982) A dynamic model for a healing fractured tibia. In Biomechanics: principles and applications (Eds R. Huiskes, D. H. Van Campen and J. R. DeWijn) 213-218 (Martinus Nijhoff, The Hague).
61. Cornelissen, M., Van der Perre, G., Martens, G. and Mulier, J. C. (1984) Vibration measurements correlated with mechanical stability characteristics. In Advances in biomaterials, biomechanics and biomaterials 83 (Eds P. Ducheyne, G. Van der Perre and A. Aubert) 127-132 (Elsevier, Amsterdam).
62. Tsuchikane A, Nakatsuchi Y, Nomura A. (1995). The einfluence pf joints and soft tissue on the natural frequency of the human tibia using the impulse response method. Proc Instn Mech Engrs 209:149-155